ALZHEIMER'S DISEASE

The *MS4A* gene cluster is a key modulator of soluble TREM2 and Alzheimer's disease risk

Yuetiva Deming[1,2]*, Fabia Filipello[3]*, Francesca Cignarella[3]*, Claudia Cantoni[3], Simon Hsu[1], Robert Mikesell[3], Zeran Li[1], Jorge L Del-Aguila[1], Umber Dube[1], Fabiana Geraldo Farias[1], Joseph Bradley[1], John Budde[1], Laura Ibanez[1], Maria Victoria Fernandez[1], Kaj Blennow[4,5], Henrik Zetterberg[4,5,6], Amanda Heslegrave[6,7], Per M Johansson[8], Johan Svensson[9], Bengt Nellgård[10], Alberto Lleo[11,12], Daniel Alcolea[11,12], Jordi Clarimon[11,12], Lorena Rami[13], José Luis Molinuevo[13,14], Marc Suárez-Calvet[14,15,16], Estrella Morenas-Rodríguez[15,17], Gernot Kleinberger[15,17,18], Michael Ewers[19], Oscar Harari[1,20,21], Christian Haass[16,17,22], Thomas J Brett[20,23], Bruno A. Benitez[1,20,21†], Celeste M. Karch[1,20,21†‡], Laura Piccio[3,20,24†‡], Carlos Cruchaga[1,20,21]*†‡

Soluble triggering receptor expressed on myeloid cells 2 (sTREM2) in cerebrospinal fluid (CSF) has been associated with Alzheimer's disease (AD). TREM2 plays a critical role in microglial activation, survival, and phagocytosis; however, the pathophysiological role of sTREM2 in AD is not well understood. Understanding the role of sTREM2 in AD may reveal new pathological mechanisms and lead to the identification of therapeutic targets. We performed a genome-wide association study (GWAS) to identify genetic modifiers of CSF sTREM2 obtained from the Alzheimer's Disease Neuroimaging Initiative. Common variants in the membrane-spanning 4-domains subfamily A (*MS4A*) gene region were associated with CSF sTREM2 concentrations (rs1582763; $P = 1.15 \times 10^{-15}$); this was replicated in independent datasets. The variants associated with increased CSF sTREM2 concentrations were associated with reduced AD risk and delayed age at onset of disease. The single-nucleotide polymorphism rs1582763 modified expression of the *MS4A4A* and *MS4A6A* genes in multiple tissues, suggesting that one or both of these genes are important for modulating sTREM2 production. Using human macrophages as a proxy for microglia, we found that MS4A4A and TREM2 colocalized on lipid rafts at the plasma membrane, that sTREM2 increased with *MS4A4A* overexpression, and that silencing of *MS4A4A* reduced sTREM2 production. These genetic, molecular, and cellular findings suggest that MS4A4A modulates sTREM2. These findings also provide a mechanistic explanation for the original GWAS signal in the *MS4A* locus for AD risk and indicate that TREM2 may be involved in AD pathogenesis not only in *TREM2* risk-variant carriers but also in those with sporadic disease.

INTRODUCTION

In 2013, two groups independently identified a rare variant in *TREM2* (triggering receptor expressed on myeloid cells 2) (p.R47H) that increased risk for Alzheimer's disease (AD) almost threefold, making *TREM2* the strongest genetic risk factor for late-onset AD since the identification of *APOE* ε*4* 30 years earlier (*1*, *2*). *TREM2* p.R47H is also associated with clinical, imaging, and neuropathological AD phenotypes, including advanced behavioral symptoms, gray matter atrophy, and Braak staging (*3*, *4*). Additional rare variants in *TREM2* have also been associated with AD risk including p.R62H, p.H157Y, p.R98W, p.D87N, p.T66M, p.Y38C, and p.Q33X (*1*, *5*–*7*).

TREM2 encodes a protein that is part of a transmembrane receptor signaling complex essential for the immune response of myeloid cells such as microglia. TREM2 is highly and specifically expressed in microglia in the central nervous system (CNS) where it plays a key role in microglial activation, survival, and phagocytosis (*8*–*11*). Recent evidence from AD animal models suggests that TREM2 has a complex relationship with the key proteins involved in AD pathogenesis,

[1]Department of Psychiatry, Washington University School of Medicine, St. Louis, MO 63110, USA. [2]Alzheimer's Disease Research Center, University of Wisconsin School of Medicine and Public Health, Madison, WI 53792, USA. [3]Department of Neurology, Washington University School of Medicine, St. Louis, MO 63110, USA. [4]Department of Psychiatry and Neurochemistry, Institute of Neuroscience and Physiology, Sahlgrenska Academy at the University of Gothenburg, Mölndal, Sweden. [5]Clinical Neurochemistry Laboratory, Department of Neuroscience and Physiology, University of Gothenburg, Sahlgrenska University Hospital, Mölndal, Sweden. [6]Department of Neurodegenerative Disease, UCL Institute of Neurology, Queen Square, London, UK. [7]UK Dementia Research Institute at UCL, London, UK. [8]Department of Clinical Sciences Helsingborg, Lund University, Lund, Sweden. [9]Department of Internal Medicine, Institute of Medicine, Sahlgrenska Academy at the University of Gothenburg, Göteborg, Sweden. [10]Department of Anesthesiology, Sahlgrenska University Hospital, Department of Internal Medicine, Institute of Medicine, Sahlgrenska Academy at the University of Gothenburg, Göteborg, Sweden. [11]Department of Neurology, IIB Sant Pau, Hospital de la Santa Creu i Sant Pau, Universitat Autònoma de Barcelona, Barcelona, Spain. [12]Center for Networker Biomedical Research in Neurodegenerative Diseases (CIBERNED), Madrid, Spain. [13]IDIBAPS, Alzheimer's Disease and Other Cognitive Disorders Unit, Neurology Service, ICN Hospital Clinic, Barcelona, Spain. [14]Barcelonaβeta Brain Research Center, Pasqual Maragall Foundation, Barcelona, Spain. [15]Biomedical Center (BMC), Biochemistry, Ludwig-Maximilians-Universität München, Munich, Germany. [16]German Center for Neurodegenerative Diseases (DZNE), Munich, Germany. [17]Munich Cluster for Systems Neurology (SyNergy), Munich, Germany. [18]ISAR Bioscience GmbH, 2152 Planegg, Germany. [19]Institute for Stroke and Dementia Research, University Hospital, LMU, Munich, Germany. [20]Hope Center for Neurological Disorders, Washington University School of Medicine, St. Louis, MO 63110, USA. [21]NeuroGenomics and Informatics, Washington University School of Medicine, St. Louis, MO 63110, USA. [22]Chair of Metabolic Biochemistry, Biomedical Center (BMC), Faculty of Medicine, Ludwig-Maximilians-Universität München, 81377 Munich, Germany. [23]Division of Pulmonary and Critical Care Medicine, Department of Internal Medicine, Washington University School of Medicine, St. Louis, MO 63110, USA. [24]Brain and Mind Centre, University of Sydney, Sydney, NSW 2050, Australia.
*These authors contributed equally to this work.
†These authors contributed equally to this work.
‡Corresponding author. Email: karchc@wustl.edu (C.M.K.); picciol@wustl.edu (L.P.); ccruchaga@wustl.edu (C. Cruchaga)

amyloid-β (Aβ) and tau (*12*). In studies suggesting that TREM2 may be protective in AD, TREM2 has been associated with phagocytosis in the presence of Aβ (*13*). The introduction of the human *TREM2* transgene reduced pathology and rescued cognitive function in amyloid-bearing mice (*14*). A common phenotype across mouse models of amyloidosis is that reduction or loss of *Trem2* leads to fewer amyloid plaque–associated microglia, resulting in more diffuse plaques and enhanced neuritic damage (*15*–*17*). In contrast, studies of tau pathology indicate that *Trem2* deficiency protects against neurodegeneration, suggesting a detrimental role for TREM2 in the presence of tau pathology (*18*, *19*). Together, these studies demonstrate that TREM2 plays an important, yet complex, role in AD pathology.

In addition to the full-length TREM2, which makes up part of a transmembrane receptor, a soluble form of TREM2 (sTREM2) is produced by alternative splicing or proteolytic cleavage of the full-length TREM2 protein (*6*, *13*, *20*). Three distinct transcripts for *TREM2* are found in human brain tissue, including a short alternatively spliced transcript that excludes exon 4 (encoding the transmembrane domain) to produce a soluble isoform of TREM2 (*6*). Recently, a cleavage site was identified in TREM2, which can be targeted by proteases such as ADAM10, ADAM17, and γ-secretase to generate sTREM2 (*21*, *22*). sTREM2 is released into the cerebrospinal fluid (CSF) where it can be quantified (*13*, *23*–*28*). CSF sTREM2 is hypothesized to increase in response to microglial activation due to neurodegenerative processes (*24*, *27*). Our group and others have demonstrated that CSF sTREM2 is elevated in AD (*23*, *24*, *26*). Changes in CSF sTREM2 appear to occur after amyloid accumulation, beginning about 5 years before clinical symptom onset in autosomal dominant forms of AD (*25*). In addition, CSF sTREM2 positively correlates with CSF tau and phosphorylated tau (ptau), but not with CSF $A\beta_{42}$, suggesting that sTREM2 may be associated with pathological processes occurring after the accumulation of Aβ (*23*, *24*, *26*). Thus, CSF sTREM2 has emerged as an important and dynamic biomarker of disease processes throughout AD pathogenesis.

Our group and others have shown that using CSF biomarkers of complex diseases as quantitative endophenotypes can help identify genes that contribute to key biological pathways involved in disease (*29*–*31*). In this study, we aimed to identify genetic modifiers of CSF sTREM2. We conducted a genome-wide association study (GWAS) of CSF sTREM2 from more than 1390 individuals and detected a locus within the membrane-spanning 4-domains subfamily A (*MS4A*) gene region (11q12.2) that displayed genome-wide significant association with CSF sTREM2. We then used bioinformatic, transcriptomic, and cellular approaches to examine correlations between *MS4A* genes and *TREM2*.

RESULTS

The goal of this study was to identify genetic modifiers of CSF sTREM2 and to better understand the role of sTREM2 in biological pathways relevant to AD. To accomplish this goal, we analyzed genetic data and CSF sTREM2 from 813 individuals from the Alzheimer's Disease Neuroimaging Initiative (ADNI). We then sought to replicate our findings in independent datasets ($n = 580$).

CSF sTREM2 concentrations correlate with age, sex, and AD biomarkers

Our discovery cohort was obtained from ADNI ($n = 813$), the largest dataset for CSF sTREM2 samples to date. The analyzed dataset included samples from 172 AD, 169 cognitively normal, 183 early mild cognitive impairment (EMCI), 221 late MCI (LMCI), and 68 significant memory concern (SMC) individuals (Table 1). We excluded participants with MCI due to non-AD causes and participants carrying previously identified risk mutations in *TREM2* (Table 2 and table S1). CSF sTREM2 concentrations in our analyses approximated a normal distribution without transformation; therefore, we analyzed the raw values, unless otherwise stated.

We tested the correlation between age at the time of lumbar puncture and CSF sTREM2 concentrations and found a positive correlation, consistent with our previous reports (Pearson $r = 0.270$, $P = 4.66 \times 10^{-15}$; fig. S1) (*24*). We also evaluated whether CSF sTREM2 was associated with sex, as previously reported (*24*–*26*, *32*). There was no significant difference between CSF sTREM2 concentrations in males (3926 ± 1969 pg/ml) versus females (3873 ± 1856 pg/ml; one-tailed $P = 0.694$; fig. S1). CSF sTREM2 concentrations positively correlated with CSF tau ($r = 0.377$, $P = 9.59 \times 10^{-29}$) and ptau ($r = 0.348$, $P = 2.08 \times 10^{-24}$; fig. S1). Consistent with our previous findings, there was no significant correlation between CSF sTREM2 concentrations and CSF $A\beta_{42}$ concentrations ($r = 0.074$, $P = 0.052$; fig. S1). CSF sTREM2 concentrations did significantly correlate with the tau/$A\beta_{42}$ and ptau/$A\beta_{42}$ ratios ($r = 0.171$, $P = 5.71 \times 10^{-6}$ and $r = 0.176$, $P = 3.18 \times 10^{-6}$, respectively). However, the correlations were not as strong as those observed between CSF sTREM2 and tau or ptau, suggesting that the correlations may be driven by the associations with CSF tau and ptau (fig. S1).

We also measured CSF sTREM2 concentrations in 38 individuals who were heterozygous for *TREM2* risk variants and were not included in the GWAS: p.D87N, p.L211P, p.R47H, p.R62H, and p.H157Y (Table 2). There was a significant difference in CSF sTREM2 concentrations among *TREM2* risk variant carriers ($P = 0.042$), as reported previously (*24*). We also observed variant-specific effects on CSF sTREM2 concentrations. CSF sTREM2 concentrations were significantly lower in p.L211P carriers (2578 ± 1444 pg/ml) compared to noncarriers (3903 ± 1919 pg/ml; $P = 0.026$; fig. S2). CSF sTREM2 concentrations were significantly elevated in p.R47H carriers (4852 ± 1172 pg/ml) compared to p.L211P carriers ($P = 0.029$) and p.D87N carriers (2082 ± 239 pg/ml; $P = 0.041$), but were not significantly different from noncarriers ($P = 0.223$; fig. S2).

The *MS4A* gene region is associated with CSF sTREM2 concentrations

To identify genetic variants that modify CSF sTREM2 concentrations, we tested for association between CSF sTREM2 concentrations and single-nucleotide polymorphisms (SNPs) with a minor allele frequency (MAF) of >0.02 using an additive linear regression model with age, sex, and two principal components as covariates. A total of 7,320,475 genotyped and imputed SNPs passed strict quality control (QC) as described in Materials and Methods. *TREM2* risk-variant carriers were excluded from the GWAS analyses.

A genome-wide significant genetic association with CSF sTREM2 was identified on chromosome 11 within the *MS4A* gene region (Fig. 1, fig. S3, and table S2). The top SNP was rs1582763, an intergenic variant nearest *MS4A4A* (located 26 kb 5′ of *MS4A4A*; 11q12.2). This common variant (A allele, MAF = 0.368, genotyped) produced a genome-wide significant association with CSF sTREM2 concentrations ($n = 807$, $\beta = 735.1$, $P = 1.15 \times 10^{-15}$; Fig. 1) and explained more than 6% of the variance in sTREM2 concentrations (adjusted $r^2 = 0.064$). Results from case-control stratified analyses indicated that both clinically diagnosed cognitively impaired individuals ($n = 606$, $\beta = 675.8$, $P = 8.19 \times 10^{-10}$) and cognitively normal controls ($n = 207$,

Table 1. ADNI cohort characteristics and CSF samples. Disease status is based on diagnosis at lumbar puncture (LP). AD, Alzheimer's disease case; Controls, cognitively healthy individuals; EMCI, early mild cognitive impairment (MCI); LMCI, late MCI; SMC, significant memory concern. Age is age at lumbar puncture; values are reported in years (mean ± SD). CDR is the clinical dementia rating (CDR) at lumbar puncture: 0 = no cognitive impairment, 0.5 = very mild cognitive impairment, and 1 = mild cognitive impairment. WashU sTREM2 represents the ADNI CSF sTREM2 values measured at Washington University. LMU sTREM2 represents the ADNI CSF sTREM2 values measured at Ludwig-Maximilians-Universität. All CSF values are represented as picograms per milliliter (mean ± SD).

	AD	Controls	EMCI	LMCI	SMC	*P*
N (813)	172	169	183	221	68	
Age	74.39 ± 8.56	74.47 ± 5.85	71.23 ± 7.39	73.06 ± 7.41	71.58 ± 5.57	<0.001
Females (%)	74 (43.0)	80 (47.3)	77 (42.1)	91 (41.2)	38 (55.9)	0.224
APOE $\varepsilon4^+$ (%)	115 (66.9)	40 (23.7)	87 (47.5)	129 (58.4)	24 (35.3)	<0.001
CDR at LP (%)						<0.001
0	0 (0.0)	169 (100.0)	0 (0.0)	1 (0.5)	68 (100.0)	
0.5	74 (43.0)	0 (0.0)	183 (100.0)	219 (99.1)	0 (0.0)	
1	98 (57.0)	0 (0.0)	0 (0.0)	1 (0.5)	0 (0.0)	
WashU sTREM2	2433.99 ± 776.77	2436.56 ± 768.94	2391.85 ± 728.48	2401.97 ± 711.59	2444.99 ± 690.01	0.964
LMU sTREM2	4018.65 ± 1946.09	3988.02 ± 1923.06	3741.56 ± 2066.17	3918.40 ± 1828.83	3784.28 ± 1724.71	0.641
CSF $A\beta_{42}$	626.69 ± 247.96	1059.19 ± 358.69	941.90 ± 367.92	747.16 ± 304.79	1115.83 ± 366.22	<0.001
CSF tau	367.80 ± 149.72	232.57 ± 81.04	262.10 ± 132.04	310.72 ± 126.60	240.33 ± 90.54	<0.001
CSF $ptau_{121}$	36.88 ± 16.49	21.21 ± 8.01	24.90 ± 14.87	30.64 ± 14.40	22.04 ± 9.39	<0.001

β = 912.4, $P = 5.20 \times 10^{-8}$) contributed to the association between the *MS4A* locus and CSF sTREM2 concentrations (fig. S4). No common variants that modified CSF sTREM2 concentrations and reached genome-wide significant *P* values in the *APOE*, *TYROBP*, *TREM2*, *ADAM10*, or *ADAM17* regions were identified (fig. S5). Common variants within the *TREM* family gene locus showed a marginal association with CSF sTREM2 concentrations (rs200443049, intronic indel, $n = 805$, β = 416.5, $P = 2.01 \times 10^{-5}$; fig. S5).

To determine whether there was more than one independent signal within the *MS4A* locus, we performed conditional analyses including rs1582763 in the regression model. In these analyses, we included rs1582763 in the model to determine whether there were independent signals beyond rs1582763. After conditioning for rs1582763 by adding the SNP genotype to the linear model as a covariate, the most significant variant was rs6591561 (G allele, MAF = 0.316, genotyped), a missense variant within *MS4A4A* (NP_076926.2:p.M159V), which was not in linkage disequilibrium with rs1582763 ($r^2 = 0.112$, $D' = 0.646$). Rs6591561 (*MS4A4A* p.M159V) was associated with CSF sTREM2 concentrations but in the opposite direction to the main signal (rs1582763). The minor allele of rs6591561 was associated with reduced CSF sTREM2 concentrations, and this association was independent of rs1582763 (before conditioning: β = −783.7, $P = 1.47 \times 10^{-9}$; after conditioning: β = −378.4, $P = 1.55 \times 10^{-4}$; Fig. 1). After conditioning for rs6591561 (*MS4A4A* p.M159V), rs1582763 remained genome-wide significant (β = 625.7, $P = 4.52 \times 10^{-11}$; Fig. 1), providing further evidence that these were independent signals.

Replication in independent datasets and meta-analysis

To replicate the associations of rs1582763 and rs6591561(*MS4A4A* p.M159V) in an independent dataset, we analyzed an additional 580 CSF sTREM2 samples along with associated genetic data that were obtained from six different studies: the Charles F. and Joanne Knight Alzheimer's Disease Research Center (Knight ADRC), the Dominantly Inherited Alzheimer's Network (DIAN), two studies from the Sahlgrenska Academy at the University of Gothenburg [GHDEM study (Growth Hormone, and related hormones, and Dementia study) and GHPH], the Memory Unit and Alzheimer's laboratory at the Hospital of Sant Pau in Barcelona [Sant Pau Initiative on Neurodegeneration (SPIN)], and the ICN Hospital Clinic-IDIBAPS in Barcelona. These datasets have been described previously (table S3) (*24*–*26*, *32*).

Analysis of CSF samples from these six datasets replicated the association of rs1582763 with CSF sTREM2 ($z = 5.743$, $P = 9.28 \times 10^{-9}$; Fig. 2). In these independent datasets, the association of the *MS4A4A* coding variant rs6591561, p.M159V, with CSF sTREM2 concentrations was also replicated ($z = -3.715$, $P = 2.03 \times 10^{-4}$; Fig. 2). Further meta-analysis combining ADNI CSF samples and CSF samples from the replication datasets showed a strong association between rs1582763 and elevated CSF sTREM2 ($P_{meta} = 4.48 \times 10^{-21}$; Fig. 2). In the meta-analysis, rs6591561 also showed a genome-wide significant association ($P_{meta} = 1.65 \times 10^{-11}$; Fig. 2). Individual results for each dataset are shown in table S4.

Variance in CSF sTREM2 concentrations explained by an *MS4A* GWAS signal

The genetic effect of rs1582763 explained more than 6% of the variance in CSF sTREM2 concentrations (adjusted $r^2 = 0.064$). Because rs6591561 may tag an independent signal within the *MS4A* locus, we added rs6591561 to the model. Both rs6591561 (β = −0.174, $P = 1.59 \times 10^{-3}$) and rs1582763 (β = 0.318, $P = 1.50 \times 10^{-9}$) were significantly associated with CSF sTREM2 concentrations, and the added genetic effect explained another 1% of the variance in CSF sTREM2 concentrations (combined SNP adjusted $r^2 = 0.075$).

Association of *MS4A* SNPs and *APOE* genotype with CSF sTREM2 and $A\beta_{42}$ concentrations

The *APOE* genotype is the strongest genetic risk factor for AD (*33*), and *APOEε4* is the strongest genetic association for increased $A\beta_{42}$ and tau in CSF (*31*, *34*). To determine whether the *APOE* genotype

Table 2. ADNI cohort characteristics, *TREM2* mutation carriers, and CSF samples. Each column is a *TREM2* variant that has been associated with AD risk and was present in the available ADNI data. *P* is the *P* value for an analysis of variance (ANOVA) comparing all the variants. Age represents age at lumbar puncture. Values represent years (mean ± SD). CDR is the clinical dementia rating at lumbar puncture. WashU sTREM2 are CSF sTREM2 ADNI values measured at Washington University. LMU sTREM2 are CSF sTREM2 ADNI values measured at Ludwig-Maximilians-Universität. All the CSF values are represented as picograms per milliliter (mean ± SD).

	p.R62H	p.R47H	p.L211P	p.D87N	p.H157Y	*P*
N	18	4	11	4	1	
Age	75.01 ± 6.48	73.24 ± 14.51	72.78 ± 4.36	71.14 ± 5.95	73.10 ± NA	0.843
Females (%)	9 (50.0)	2 (50.0)	6 (54.5)	0 (0)	1 (100.0)	0.393
APOE ε4$^+$ (%)	7 (38.9)	3 (75.0)	2 (18.2)	2 (50.0)	0 (0)	0.194
CDR at LP (%)						0.815
0	4 (22.2)	1 (25.0)	5 (45.5)	1 (25.0)	1 (100.0)	
0.5	10 (55.6)	3 (75.0)	5 (45.5)	3 (75.0)	–	
1	4 (22.2)	–	–	–	–	
2	–	–	1 (9.1)	4 (0.7)	–	
Case status						0.871
AD	13 (72.2)	2 (50.0)	6 (54.5)	1 (25.0)	–	
CO	3 (16.7)	1 (25.0)	3 (27.3)	1 (25.0)	1 (100.0)	
WashU sTREM2	2153 ± 842.34	2573 ± 237.61	1636 ± 563.94	1570 ± 162.55	3658.23 ± NA	0.140
LMU sTREM2	3335 ± 1882	4791 ± 965.51	2386 ± 1389	1615 ± 757.86	5641.71 ± NA	0.055
CSF $A\beta_{42}$	976.76 ± 381.52	828.13 ± 351.90	1076 ± 507.09	685.67 ± 251.93	NA	0.443
CSF tau	303.46 ± 135.43	307.85 ± 97.93	246.24 ± 113.22	252.97 ± 122.51	213.70 ± NA	0.678
CSF $ptau_{121}$	29.31 ± 14.86	30.80 ± 13.93	22.18 ± 12.66	23.42 ± 12.99	18.05 ± NA	0.729

is associated with CSF sTREM2, we created a variable representing *APOE*-mediated AD risk by recoding *APOE* genotype for each individual as 0 for ε*2*/ε*2*, 1 for ε*2*/ε*3*, 2 for ε*3*/ε*3*, 3 for ε*2*/ε*4*, 4 for ε*3*/ε*4*, and 5 for ε*4*/ε*4*. We added this *APOE* genotype risk variable to a regression model, adjusting for age, sex, and two principal components for population stratification, and found that *APOE* genotype was not significantly associated with CSF sTREM2 ($\beta = -26.5$, $P = 0.613$). The SNP commonly used as a proxy for *APOE* ε*4*, rs769449, was also not associated with CSF sTREM2 ($\beta = -106.9$, $P = 0.308$).

The influence of *APOE* genotype on Aβ pathology, including CSF $A\beta_{42}$ concentration, has been a consistent finding (*31*, *35*). Of the 813 individuals in this study, we had data for CSF $A\beta_{42}$ concentrations available for 695 individuals. To compare CSF $A\beta_{42}$ and sTREM2 concentrations on the same scale, we converted $A\beta_{42}$ and sTREM2 values to *z*-scores by subtracting the mean and dividing by the SD for each respective protein. After conversion, we verified the association between *APOE* genotype and CSF $A\beta_{42}$. As expected, there was a strong negative effect of *APOE* genotype on CSF $A\beta_{42}$ ($\beta = -0.361$, $P = 1.69 \times 10^{-34}$). We also stratified the CSF $A\beta_{42}$ into quartiles and calculated the odds ratio (OR) of *APOE* genotype for the first quartile versus the last quartile. *APOE* genotype had an OR of 2.84 for lower CSF $A\beta_{42}$ concentrations [95% confidence interval (CI), 2.30 to 3.56; $P = 8.44 \times 10^{-21}$].

Within the same subset of individuals, the effect size of rs1582763 on CSF sTREM2 concentration was similar ($\beta = 0.366$, $P = 7.53 \times 10^{-13}$) to that of *APOE* on CSF $A\beta_{42}$ concentration ($\beta = -0.361$, $P = 1.69 \times 10^{-34}$). When comparing the lower versus upper quartiles of CSF sTREM2, rs1582763 had an OR of 3.34 for higher CSF sTREM2 (95% CI, 2.37 to 4.82; $P = 2.50 \times 10^{-11}$), which was similar to the magnitude of effect of *APOE* on CSF $A\beta_{42}$ (OR, 2.84; 95% CI, 2.30 to 3.56). Thus, the impact of rs1582763 (located in the *MS4A* gene region) on CSF sTREM2 concentration was similar to that of *APOE* (the major modulator of AD risk) on CSF $A\beta_{42}$ concentration.

Additional genes associated with CSF sTREM2 concentrations

To identify genes associated with CSF sTREM2 concentration, we used MAGMA (Multi-marker Analysis of GenoMic Annotation), which maps every SNP to the nearest gene, takes into account linkage disequilibrium structure, and uses multiple regression analyses to provide a *P* value for the association of each gene with the tested phenotype. There were four genes associated with CSF sTREM2 concentration that passed multiple test correction ($P < 2.75 \times 10^{-6}$). All of these genes belonged to the *MS4A* gene family: *MS4A4A* ($P = 3.15 \times 10^{-11}$), *MS4A4E* ($P = 6.13 \times 10^{-12}$), *MS4A2* ($P = 1.29 \times 10^{-11}$), and *MS4A6A* ($P = 1.44 \times 10^{-11}$; Fig. 3). The gene encoding the TREM-like transcript 2 (*TREML2*), which is structurally similar to TREM2 but does not associate with DAP12, approached gene-wide significance with 89 mapped variants ($P = 3.23 \times 10^{-6}$; Fig. 3), suggesting that there may be additional genes contributing to changes in CSF sTREM2 concentration.

Shared genetic architecture between sTREM2, AD risk, and age at onset

To determine the extent to which genetic architecture is shared between AD risk and CSF sTREM2, we used PRSice to calculate the polygenic risk score (PRS) from summary statistics obtained from the IGAP (International Genomics of Alzheimer's Project) AD risk

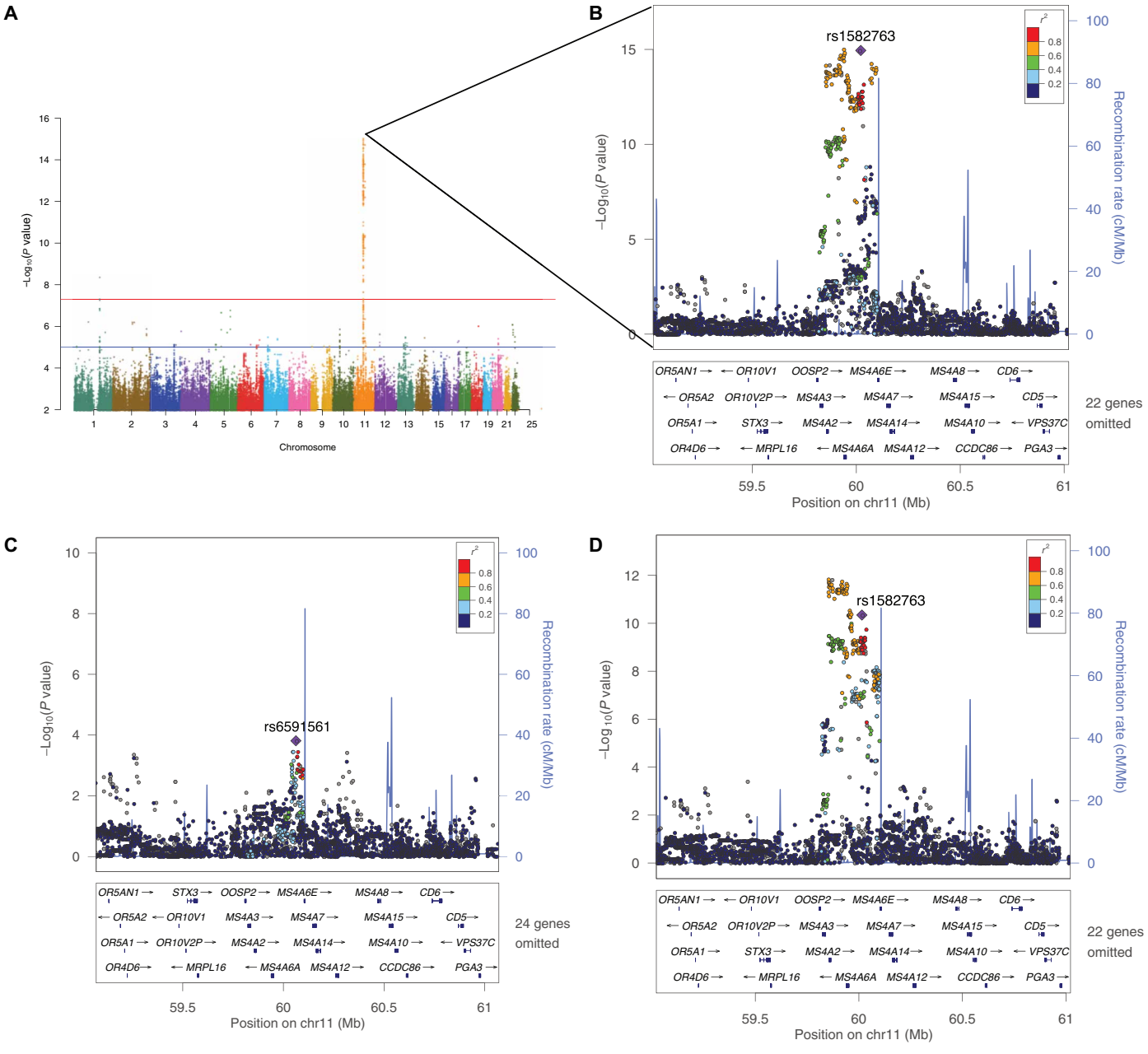

Fig. 1. Association plots from single-variant analysis of CSF sTREM2 samples. (**A**) Manhattan plot shows the negative $\log_{10}$-transformed *P* values on the *y* axis for CSF sTREM2 concentrations based on measurements of ADNI CSF samples by Ludwig-Maximilians-Universität. Comparable results were found with measurements of ADNI CSF samples by Washington University (fig. S3). The horizontal lines represent the genome-wide significance threshold (red) and suggestive threshold (blue). (**B**) Regional association plot of the *MS4A* gene region in the single-variant analysis. (**C**) Regional association plot of the *MS4A* region after conditioning on the top SNP (rs1582763). In this analysis, rs1582763 was included in the model to identify additional independent signals. (**D**) Regional association plot of the *MS4A* region after conditioning on SNP rs6591561 (*MS4A4A* p.M159V). The SNPs for each regional plot are represented by a purple diamond. Each dot represents individual SNPs, and dot colors in the regional plots represent linkage disequilibrium with the named SNP. Blue vertical lines in the regional plots show recombination rate as marked on the right-hand *y* axis.

meta-analysis (*36*), after calculating the optimum *P* value threshold and regressing the PRS against CSF sTREM2. After testing >6 million SNPs that were found in both the IGAP summary statistics and the genetic data from ADNI, less than 0.5% of the variability of CSF sTREM2 was explained by AD risk variants with $P < 6 \times 10^{-4}$ ($r^2 = 4.97 \times 10^{-3}$, $P = 0.034$). To determine how much of this was explained by the shared signal in the *MS4A* region, we removed SNPs located between the 59.5– and 60.5–base pair region on chromosome 11 and repeated the analyses. The results were similar with <0.4% of the variability explained by AD risk variants with $P < 6 \times 10^{-4}$ ($r^2 = 3.92 \times 10^{-3}$, $P = 0.060$), suggesting that although the shared association between the *MS4A* region, AD risk, and sTREM2 explained approximately 0.1% of the variance of CSF sTREM2 concentration, there may be some other AD risk variants associated with CSF sTREM2 as well.

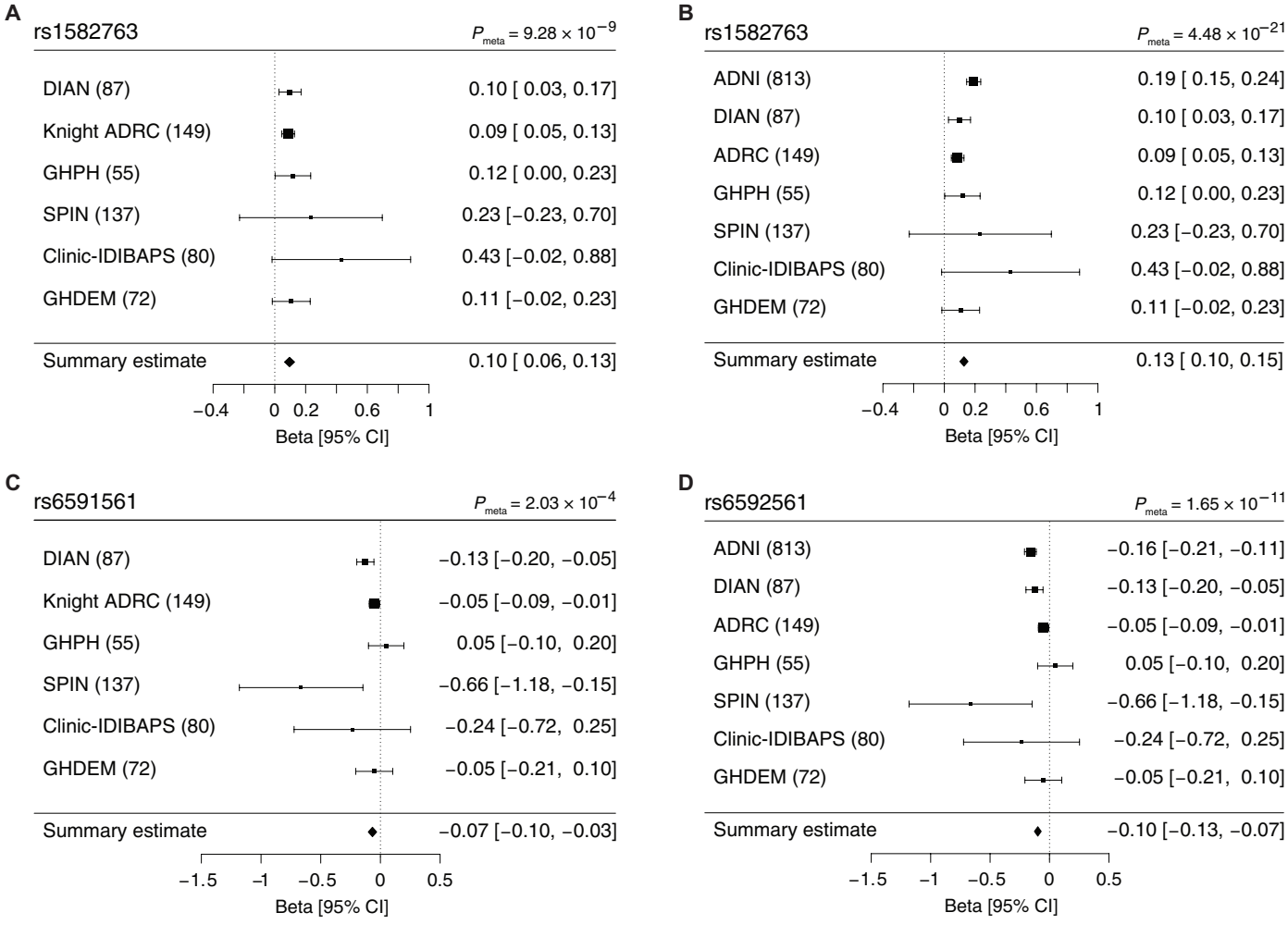

Fig. 2. Meta-analysis of replication datasets. (**A**) Forest plot of the meta-analysis of rs1582763 in the replication datasets from the DIAN, Knight ADRC, GHPH, SPIN, Clinic-IDIBAPS, and GHDEM cohorts. (**B**) Forest plot of the meta-analysis of rs1582763 including CSF samples from the ADNI cohort. (**C**) Forest plot of *MS4A4A* p.M159V (rs6591561) in the meta-analysis including CSF samples from the DIAN, Knight ADRC, GHPH, SPIN, Clinic-IDIBAPS, and GHDEM cohorts. (**D**) Forest plot of *MS4A4A* p.M159V (rs6591561) in the meta-analysis including CSF samples from the cohorts shown in (C) and the ADNI cohort. The sample size (*n*) for each study is in parentheses next to the study name.

Determining whether sTREM2 is involved in AD pathogenesis

Next, we used Mendelian randomization to determine whether CSF sTREM2 is involved in AD pathogenesis or whether it is just associated with disease due to either a confounding factor or reverse causality. Mendelian randomization is a method that uses genetic variation to estimate a causal effect from observational data, in this case CSF sTREM2 concentrations, in the presence of confounding factors. We used the two independent genome-wide SNPs in chromosome 11 (rs1582763 and rs6591561) as instrumental factors. We also used the top SNP in chromosome 6 (rs28385608), given that this locus was marginally significant in both the single-variant and gene-based analyses. Summary statistics from the largest AD risk GWAS published to date (*36*) were used as input data. We ran multiple Mendelian randomization models to take into account any potential heterogeneity in the data and to obtain robust estimates. For example, the penalized MR-Egger method downweights the variants with heterogeneous causal estimates. In all Mendelian randomization models, the analyses yielded a significant association ($P \leq 2.14 \times 10^{-3}$; Fig. 4), suggesting that CSF sTREM2 may be involved in AD pathogenesis.

Functional annotation of the *MS4A* gene region

The genome-wide significant association with CSF sTREM2 was located in a gene-rich region including at least 15 genes, most of which are members of the *MS4A* gene family. These genes include *OOSP2*, *OOSP4B*, *OOSP1*, *MS4A2*, *MS4A6A*, *MS4A4E*, *MS4A4A*, *MS4A6E*, *MS4A7*, *MS4A14*, *MS4A5*, *MS4A1*, *MS4A12*, *MS4A13*, and *MS4A8*. To determine the functional variants and specific genes that modulate CSF sTREM2, we performed additional bioinformatic analyses.

We first examined whether any of the genome-wide significant variants were located within exonic regions. We identified two coding variants: the missense variant within *MS4A4A* rs6591561 (p.M159V; MAF = 0.316, β = −593.6, $P = 1.47 \times 10^{-9}$), which is reported above, and a synonymous variant within *MS4A6A* rs12453 (p.L137L; MAF = 0.392,

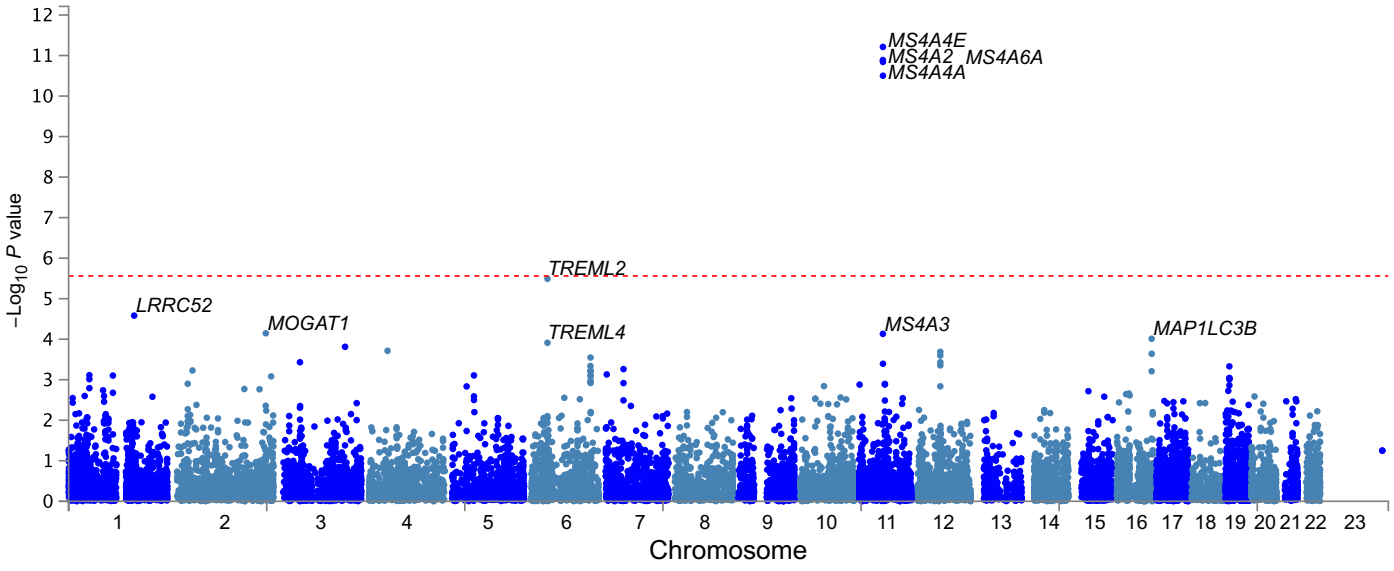

Fig. 3. Association plot from gene-based analysis for CSF sTREM2. We performed gene-based analyses using MAGMA to identify genes associated with CSF sTREM2 concentrations. Manhattan plot shows the negative $\log_{10}$-transformed *P* values on the *y* axis. Each dot represents one gene; the top 10 genes in the MAGMA results are labeled. The red dashed line represents the gene-wide significance threshold ($P = 2.74 \times 10^{-6}$).

β = 710.5, $P = 1.77 \times 10^{-15}$), which is in high linkage disequilibrium with rs1582763 ($r^2 = 0.782$, $D' = 0.924$). Neither variant was predicted by SIFT (Sorting Intolerant From Tolerant; https://sift.bii.a-star.edu.sg/) or PolyPhen to be loss of function, pathogenic, or damaging.

Because the top signal, rs1582763, was independent of the *MS4A4A* coding variant, we examined whether this top variant showed evidence of expression quantitative trait locus (eQTL) effects on *MS4A* genes. We queried the Blood eQTL browser from Westra (www.genenetwork.nl/bloodeqtlbrowser/), eQTL data from the Genotype-Tissue Expression (GTEx) project (https://www.gtexportal.org/home/), and eQTL data from the Brain eQTL Almanac (Braineac) (www.braineac.org). In human whole blood, rs1582763 was associated with reduced expression of *MS4A6A* (GTEx: β = −0.089, $P = 3.90 \times 10^{-5}$; Westra: $Z = -23.42$, $P = 2.95 \times 10^{-121}$) and *MS4A4A* (GTEx: β = −0.123, $P = 6.1 \times 10^{-5}$; Westra: $Z = -7.21$, $P = 5.52 \times 10^{-13}$) and increased expression of *MS4A2* (Westra: $Z = 8.06$, $P = 7.49 \times 10^{-16}$). To verify these findings, we analyzed gene expression data from blood obtained from 365 individuals in the ADNI dataset. We found that rs1582763 produced a cis-eQTL effect with reduced *MS4A4A* expression (β = −0.226, $P = 1.04 \times 10^{-4}$) and reduced *MS4A6A* expression (β = −0.080, $P = 6.02 \times 10^{-6}$). The eQTL effect of rs1582763 on *MS4A4A* and *MS4A6A* was observed in both clinically diagnosed AD cases ($n = 235$; *MS4A4A*: β = −0.194, $P = 6.05 \times 10^{-3}$; *MS4A6A*: β = −0.053, $P = 1.24 \times 10^{-2}$) and cognitively normal control individuals ($n = 80$; *MS4A4A*: β = −0.326, $P = 1.10 \times 10^{-2}$; *MS4A6A*: β = −0.138, $P = 3.32 \times 10^{-4}$), suggesting that the cis-eQTL effect was independent of disease status.

We further analyzed whether rs1582763 produced an eQTL effect in human brain tissue using GTEx and Braineac data. The GTEx project is an ongoing effort to build a comprehensive public resource to study tissue-specific gene expression and regulation. Samples were collected from 53 nondiseased tissue sites, including brain, across nearly 1000 individuals (https://gtexportal.org/home/). Braineac is a database that includes gene expression and genetic data in 10 different brain regions from 134 brains free of neurodegenerative disease (http://braineac.org/). Rs1582763 was nominally associated with *MS4A4A* expression in cortex of human brain tissue samples from both GTEx (β = 0.215, $P = 8.0 \times 10^{-3}$) and Braineac (β = 0.327, $P = 6.3 \times 10^{-3}$; tables S5 and S6). However, the direction of the eQTL effect in brain was opposite to the effect in blood. Similarly, rs1582763 produced a nominal cis-eQTL effect on *MS4A6A* expression in GTEx (frontal cortex: β = 0.183, $P = 0.04$; cortex: β = 0.165, $P = 0.05$) and Braineac (medulla: β = 0.337, $P = 4.50 \times 10^{-4}$) human brain tissue samples. These data suggest that there may be tissue-specific effects of rs1582763 on the expression of *MS4A* genes. These results also suggest that *MS4A4A* and *MS4A6A* genes modulate CSF sTREM2 concentrations.

To determine whether rs1582763 produced a trans-eQTL effect on *TREM2* expression in brain tissue, we analyzed genetic and expression data in the Knight ADRC and Mount Sinai Brain Bank human brain tissue samples (*37*). Rs1582763 was not associated with *TREM2* gene expression (Knight ADRC: parietal lobe, $P = 0.610$; Mount Sinai Brain Bank: Brodmann area 10, $P = 0.251$; Brodmann area 22, $P = 0.635$; Brodmann area 36, $P = 0.269$; and Brodmann area 44, $P = 0.999$). These findings suggest that the association between rs1582763 and CSF sTREM2 is driven by the cis-eQTL effect on *MS4A4A* and *MS4A6A* rather than directly affecting *TREM2* expression.

MS4A gene expression and *TREM2* gene expression are highly correlated

To begin to understand the relationship between *MS4A* genes and *TREM2*, we examined the correlation between expression of *TREM2* and expression of genes within the *MS4A* cluster using brain RNA sequencing (RNA-seq) data. Among the 16 genes tested from the *MS4A* gene cluster, the expression of three genes (*MS4A4A*, *MS4A6A*, and *MS4A7*) was consistently positively correlated with *TREM2* gene expression in human brain tissue. In autopsy-confirmed late-onset AD cases and controls (from the Knight ADRC dataset), *TREM2*

A

Mendelian randomization analyses for CSF sTREM2 vs. AD risk

Method	Estimate	SE	95% CI		*P*
MR-Egger	-3.35×10^{-04}	7.26×10^{-05}	-4.77×10^{-04}	-1.92×10^{-04}	3.97×10^{-06}
Penalized MR-Egger	-3.35×10^{-04}	7.26×10^{-05}	-4.77×10^{-04}	-1.92×10^{-04}	3.97×10^{-06}
Robust MR-Egger	-3.35×10^{-04}	1.93×10^{-05}	-3.73×10^{-04}	-2.97×10^{-04}	$<1.00 \times 10^{-06}$
Penalized robust MR-Egger	-3.35×10^{-04}	1.93×10^{-05}	-3.73×10^{-04}	-2.97×10^{-04}	$<1.00 \times 10^{-06}$

B

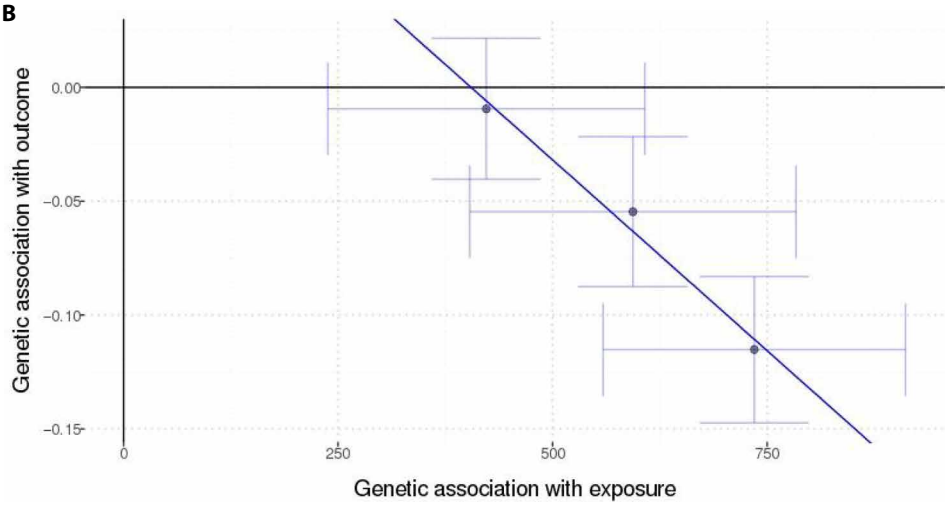

Fig. 4. Mendelian randomization analyses for CSF sTREM2 versus AD risk. (**A**) Summary statistics for the different Mendelian randomization (MR) models analyzed. Residual SE is 0.934. Residual SE is set to 1 in calculations of CI when its estimate is less than 1. Heterogeneity test statistic is 0.3884 on one degree of freedom ($P = 0.533$). I^2_GX statistic is 60.0%. (**B**) Scatterplot illustrating genetic associations with AD risk (outcome) against genetic associations with CSF sTREM2 concentrations, with error bars representing 95% CIs for the associations. The variants are all oriented to the CSF sTREM2 effect. The dark blue line represents the MR-Egger causal estimate.

expression was significantly correlated with expression of *MS4A4A* ($n = 40$, $r = 0.41$, $P = 8.00 \times 10^{-3}$) and *MS4A6A* ($n = 41$, $r = 0.67$, $P = 1.60 \times 10^{-6}$; fig. S6 and table S7). These findings were replicated in two independent RNA-seq datasets obtained from the Mayo Clinic Brain Bank ($n = 162$; *MS4A4A*: $r = 0.68$, $P = 1.00 \times 10^{-23}$; *MS4A6A*: $r = 0.76$, $P = 1.60 \times 10^{-31}$; fig. S7 and table S8) and Mount Sinai Brain Bank ($n = 300$; *MS4A4A*: $r = 0.61$, $P = 1.60 \times 10^{-16}$; *MS4A6A*: $r = 0.52$, $P = 7.90 \times 10^{-8}$; fig. S8 and table S9). These data further support that *MS4A4A* and *MS4A6A* may modulate CSF sTREM2.

Targeting MS4A4A on human macrophages decreases soluble TREM2 in vitro

MS4A4A and *MS4A6A* are both highly expressed in microglia (*38*). The mouse ortholog for *MS4A6A* is *Ms4a6e*; however, there is no mouse ortholog for *MS4A4A* (*39*, *40*). Thus, to understand the role of *MS4A* genes in TREM2 function, we used human cell models. To begin evaluating the functional connection between TREM2 and MS4A4A and MS4A6A, we used human macrophages because they express TREM2, MS4A4A, and MS4A6A and are frequently used as a model of microglia (*41*). Human macrophages were derived in vitro from blood monocytes obtained from healthy individuals. The macrophage culture medium was tested for the presence of sTREM2 by enzyme-linked immunosorbent assay (ELISA). Given that stimulation of macrophages with interleukin-4 (IL-4) results in up-regulation of TREM2 and MS4A4A (*42*, *43*), we measured sTREM2 in the presence or absence of IL-4 as previously described (*27*). We detected sTREM2 in the macrophage culture media beginning at day 3 after isolation of monocytes, and sTREM2 increased progressively with time of macrophages in culture, consistent with previous reports ($P < 0.0001$; fig. S9A) (*27*). By day 7 after isolation of monocytes, stimulation with IL-4 had significantly increased sTREM2 in the culture media compared to untreated cells ($P = 0.015$; fig. S9B).

To examine the therapeutic potential of targeting these MS4A proteins, we next evaluated whether antibody-mediated targeting of MS4A4A or MS4A6A expression modulated extracellular sTREM2. Human macrophages were treated on day 7 after isolation of human monocytes with commercially available antibodies to MS4A4A or MS4A6A or were treated with an isotype antibody as control, and then sTREM2 was measured in culture media 48 hours after treatment. We found that an antibody directed against MS4A4A was sufficient to significantly reduce sTREM2 concentrations in macrophage cultures ($P < 0.0001$; Fig. 5A). However, treatment with an anti-MS4A6A antibody failed to alter sTREM2 concentrations in macrophage cultures (Fig. 5A). We observed similar results when macrophages were stimulated with IL-4 before antibody treatment ($P < 0.0001$; fig. S9C). The effect of the MS4A4A antibody on sTREM2 concentrations in human macrophage cultures was dose-dependent. Treatment of macrophages with MS4A4A antibody (1, 5, or 10 μg/ml) produced a dose-dependent decrease in sTREM2 ($P = 9.63 \times 10^{-9}$, Spearman $R^2 = -0.88$; Fig. 5). Extracellular sTREM2 concentrations were unchanged with increasing concentrations of the isotype-matched control antibody [mouse immunoglobulin G (IgG); Fig. 5B]. The slope for the anti-MS4A4A antibody was significantly different from that for the control antibody ($P = 0.0018$; Fig. 5B). These results suggest that specifically targeting MS4A4A reduced sTREM2 concentrations in human macrophages in vitro.

To determine whether *MS4A4A* expression was sufficient to alter release by macrophages of sTREM2 into culture media, we either overexpressed or knocked down human *MS4A4A* using a lentiviral system in human macrophages. For the overexpression experiments, human macrophages were transduced with lentiviral particles containing *MS4A4A* or green fluorescent protein (GFP) for 24 hours. Cells and culture media were collected 48 hours after transduction. Overexpression of wild-type *MS4A4A* was sufficient to significantly increase *MS4A4A* mRNA ($P = 0.0043$; Fig. 5C) and MS4A4A protein ($P < 0.0001$; Fig. 5D and fig. S9D) compared to macrophages treated with lentiviral particles containing GFP. Macrophages overexpressing

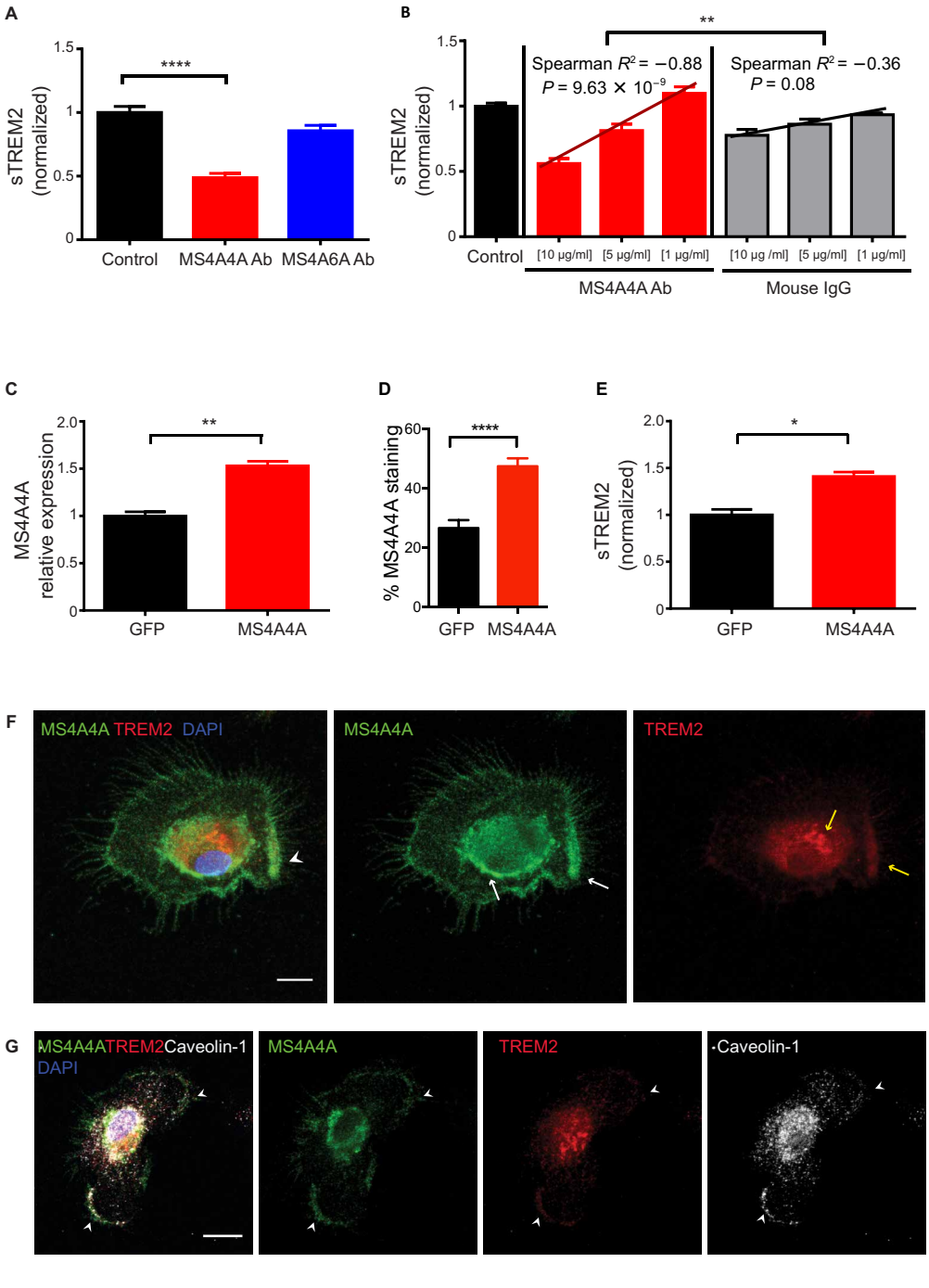

Fig. 5. sTREM2 concentrations in primary human macrophage cultures. The effects of overexpressing *MS4A4A* in primary human macrophages or treating macrophages with anti-MS4A4A antibody on sTREM2 concentrations in culture media were measured. (**A**) sTREM2 was measured in cell culture medium 48 hours after treatment of primary human macrophages with antibodies against MS4A4A and MS4A6A. sTREM2 normalized values are shown; sTREM2 was normalized based on the average concentration for the control in each experiment. Error bars represent means ± SEM. ****$P < 0.0001$. P values were calculated using the Mann-Whitney test. (**B**) Dose-response effect of anti-MS4A4A antibody (Ab) or an isotypic control mouse IgG on sTREM2 production by primary human macrophages in vitro. Difference in the slope between the dose-response for anti-MS4A4A antibody and mouse IgG isotype antibody control was tested using ANOVA. **$P < 0.01$. Four experiments were performed; results for sTREM2 concentrations in cell culture supernatants are expressed as normalized values relative to untreated controls. (**C**) *MS4A4A* was overexpressed in primary human macrophages using a lentiviral vector encoding the human *MS4A4A* cDNA (NM_148975). The plot represents mRNA expression relative to *GAPDH*. Error bars represent means ± SD. **$P < 0.01$. P values were calculated by Mann-Whitney test. (**D**) Quantification of MS4A4A expression by immunofluorescence in control primary human macrophages expressing green fluorescent protein (GFP) or human macrophages overexpressing MS4A4A. MS4A4A expression was analyzed as the percentage area of positive staining (number of positive pixels/1 mm^2) within the area of interest. ****$P < 0.0001$. (**E**) sTREM2 concentration in cell culture supernatants from primary human macrophages overexpressing *MS4A4A* normalized to that for control macrophages expressing GFP. *$P < 0.05$. P values were calculated using the Mann-Whitney test. (**F**) Representative confocal microscopy images of human macrophages immunostained with antibodies against TREM2 (red) and MS4A4A (green). White arrows indicate an MS4A4A-positive signal, whereas yellow arrows indicate a TREM2-positive signal. White arrowheads indicate colocalizing signals for TREM2 and MS4A4A on the macrophage plasma membrane. Scale bar, 10 μm. DAPI, 4′,6-diamidino-2-phenylindole. (**G**) Representative confocal microscopy images of primary human macrophages immunostained with antibodies against caveolin-1 (gray), TREM2 (red), and MS4A4A (green). White arrowheads indicate colocalization signals. Scale bar, 10 μm.

MS4A4A also produced significantly more sTREM2 compared to GFP control-treated cells ($P = 0.028$; Fig. 5E). These results were replicated in four independent experiments and demonstrate that targeting MS4A4A at the molecular or protein level was sufficient to alter sTREM2 concentrations in macrophage culture media. Conversely, transduction of human macrophages with lentiviral particles containing *MS4A4A*-specific short hairpin RNA (shRNA) decreased *MS4A4A* expression by 75% ($P = 0.01$; fig. S10) and was sufficient to reduce sTREM2 concentrations compared to macrophages treated with scrambled shRNA as a control ($P = 0.0001$; fig. S10).

MS4A4A colocalizes with TREM2 in human macrophages

We performed immunocytochemistry studies in human macrophages to determine the cellular localization of MS4A4A and TREM2.

MS4A4A is reportedly expressed on the macrophage plasma membrane (*42*) and on the plasma membrane and intracellular organelles in human mast cells, where it may play a role in protein trafficking (*44*). Consistent with these reports, we found MS4A4A primarily expressed on the plasma membrane of human macrophages in vitro and also intracellularly (Fig. 5F, white arrows). Intense staining for TREM2 was detected in areas surrounding the nucleus and in discrete regions on the plasma membrane (Fig. 5F, yellow arrows). To determine specific colocalization of MS4A4A and TREM2, we stained human macrophages with markers for the endoplasmic reticulum (KDEL), Golgi (giantin), and lipid rafts (caveolin-1) (Fig. 5G and fig. S9G). MS4A4A and TREM2 colocalized with caveolin-1–positive lipid-enriched structures on the plasma membrane (Fig. 5G, white arrowheads). We also detected partial colocalization of TREM2 with both endoplasmic reticulum (KDEL) and Golgi (Giantin). In contrast, MS4A4A did not colocalize with these intracellular markers (fig. S9G). IL-4–mediated stimulation of human macrophages increased expression of both MS4A4A and TREM2 (fig. S9, E, F and H), which is consistent with previous reports (*41*, *42*).

DISCUSSION

In this study, we performed a genome-wide analysis for genetic modifiers of sTREM2 in CSF. We observed two independent signals in the *MS4A* gene region that passed genome-wide significance thresholds for association with CSF sTREM2 concentrations: rs1582763 and rs6591561 (*MS4A4A* p.M159V). Rs1582763 is associated with elevated CSF sTREM2, reduced AD risk (*36*), and delayed age at onset (*40*). Conversely, rs6591561 (*MS4A4A* p.M159V) is associated with reduced CSF sTREM2, increased AD risk (*36*), and accelerated age at onset of AD (*40*). We show here that these SNPs modified expression of *MS4A4A* and *MS4A6A* in human peripheral blood cells and brain tissue. The expression of both these genes was highly correlated with *TREM2* gene expression. In human macrophages, MS4A4A and TREM2 colocalized on lipid rafts, and pharmacological or genetic modification of MS4A4A resulted in altered sTREM2 concentrations in macrophage culture media. Thus, we present genetic, molecular, and functional evidence suggesting that *MS4A* genes, particularly *MS4A4A*, may be key modulators of sTREM2.

Our findings that variants in the *MS4A* gene region are associated with CSF sTREM2 provide a putative biological connection between the MS4A family, TREM2, and AD risk. Before this study, *TREM2* was directly implicated in AD through the identification of rare variants that increase AD risk (*1*, *2*). Thus, TREM2 was thought to only affect a small percentage of AD cases. The putative role of TREM2 in sporadic AD was less clear. Common variants in the *MS4A* locus, including the top SNP we found associated with CSF sTREM2, were reported to be associated with AD risk (rs1582763; OR, 0.898; $P = 1.81 \times 10^{-15}$) (*36*) and age at onset [hazards ratio (HR) = 0.929, $P = 9.26 \times 10^{-9}$] (*40*), but the functional variant and mechanism of action were unknown. Here, we show that variants within this AD risk locus modify CSF sTREM2 concentrations. More specifically, our data indicate that AD risk variants are associated with lower CSF sTREM2 concentrations and that the protective AD variants are associated with elevated CSF sTREM2 concentrations. This relationship between CSF sTREM2 and AD risk is supported by previous studies suggesting that *TREM2* variants associated with AD risk or causal for Nasu-Hakola disease are loss-of-function mutations. Our findings and previous studies indicate that increasing TREM2 or activating the TREM2 signaling pathway could offer a new therapeutic approach for treating AD (*45*).

We present multiple lines of evidence that genes within the *MS4A* cluster modulate sTREM2 concentrations. First, we observed a strong and consistent association across multiple independent datasets ($P_{meta} = 4.48 \times 10^{-21}$; Fig. 2). For comparison, the effect size of rs1582763 on CSF sTREM2 (OR, 3.34; 95% CI, 2.37 to 4.82) is similar to that of the *APOE* genotype on CSF $A\beta_{42}$ (OR, 2.84; 95% CI, 2.30 to 3.50). Second, the *MS4A* association with CSF sTREM2 represents a trans effect: *TREM2* is located on chromosome 9, and this *MS4A* locus is on chromosome 11. As our group and others have reported, it is not common to find trans–protein QTLs (pQTLs) with large effect sizes and most trans-pQTLs occur in genes that encode receptors or that have other regulatory influences on the protein studied (*46*–*51*). Thus, we hypothesize that one or more genes within the *MS4A* locus may be key modulators of sTREM2. Third, our functional studies support a relationship between MS4A4A and sTREM2. Using pharmacological (antibody) or genetic (lentivirus-mediated overexpression and knockdown) approaches, we targeted MS4A4A and observed changes in sTREM2 concentrations in human macrophage cultures. Overexpression of *MS4A4A* resulted in elevated extracellular sTREM2 in human macrophage cultures compared to macrophages overexpressing GFP. Antibodies targeting MS4A4A that resulted in MS4A4A reduction led to a dose-dependent reduction in sTREM2 concentrations.

These results suggest that MS4A4A may be a therapeutic target for AD. MS4A4A colocalized with TREM2 in human macrophages, and both proteins were up-regulated in response to IL-4–mediated stimulation. *TREM2* and *MS4A4A* are both highly and specifically expressed in human microglia (*38*). Whereas the function of MS4A4A in the brain is poorly understood, it may be involved in protein trafficking and clathrin-dependent endocytosis (*44*). The finding that modifying MS4A4A affects sTREM2 in human macrophages in vitro supports a putative relationship between these two proteins. Compounds that induce overexpression of MS4A4A or increase MS4A4A activity could modify AD risk through regulation of sTREM2.

The origin and function of sTREM2 is still poorly understood. Most studies investigating the role of TREM2 in AD pathogenesis have focused on characterizing the impact of *TREM2* loss-of-function mutations or rare *TREM2* risk variants. These studies have evaluated the impact of TREM2 deficiency (*18*, *52*) or haploinsufficiency (*15*), but they are unable to draw any conclusions about a potential role for sTREM2 specifically. Some evidence suggests that sTREM2 binds to and sequesters TREM2 ligands, such as apolipoproteins, thus preventing these ligands from activating the TREM2 receptor (*53*, *54*). Others propose that sTREM2 works independently of the TREM2 receptor. Treatment with sTREM2 enhanced microglial survival and cytokine release in both wild-type and $Trem2^{-/-}$ microglia in culture (*55*). In both wild-type and $Trem2^{-/-}$ primary microglia, the introduction of sTREM2 increased mRNA expression of IL-1β, IL-6, tumor necrosis factor (TNF), and IL-10 in a dose-dependent manner, further suggesting that sTREM2 may trigger microglial activation independently of the TREM2 receptor (*55*). These findings demonstrate that further research is necessary to determine the role of sTREM2 in AD. The correlations between CSF sTREM2 and CSF tau ($r = 0.377$, $P = 9.59 \times 10^{-29}$) and CSF ptau ($r = 0.348$, $P = 2.08 \times 10^{-24}$), which have been reported consistently in independent studies (*23*, *24*, *26*), may provide some clue. There is increasing evidence that microglia play a key role in tau-mediated neurodegeneration

in AD and similar tauopathies (*56*). Considering that *TREM2*, *MS4A4A*, and *MS4A6A* are exclusively expressed in microglia in the CNS, our findings add further support to this putative role for microglia in tau-mediated pathogenic mechanisms.

Our Mendelian randomization analyses provide additional support that sTREM2 may be involved in AD pathogenesis. Mendelian randomization uses genetic variation as instrumental variables to analyze whether a specific variable, which can be a treatment or a protein (*57*), is associated with a specific outcome (AD risk in this case) independently of reverse causation or confounding effects. We used as instrumental variables the three independent SNPs that showed strong association with sTREM2 and found significant associations for CSF sTREM2 with AD risk, demonstrating that sTREM2 may be involved in AD pathogenesis and not merely a product of the disease process. In this study, we did not analyze the association of sTREM2 with AD clinical status because previous studies (*24*, *25*) have recently demonstrated that sTREM2 is associated with AD risk. Although case-control studies are informative, they do not account for longitudinal changes in biomarkers, which may change as a function of disease stage. Additional analyses demonstrating the longitudinal changes in CSF sTREM2 concentrations using the amyloid/tau/neurodegeneration (A/T/N) classification will be helpful for understanding the dynamic changes in CSF sTREM2 during the course of AD.

There are some limitations to the present study. The first limitation is that this study only included common variants (MAF > 2%); therefore, we were unable to determine the effect of genes that only harbor low frequency or rare functional variants. Although some studies have linked APOE with TREM2 (*58*), we did not observe an association between *APOE* genotype and CSF sTREM2 concentrations. Thus, *APOE* does not play a role in modulating sTREM2. However, we cannot yet conclude whether other genes such *TYROBP*, *ADAM10*, or *ADAM17* play a role in modulating CSF sTREM2. These genes were reported to be involved in TREM2 cleavage (*21*, *22*); therefore, we would expect to find a strong association with CSF sTREM2 in these gene regions. However, the risk variants in *TYROBP* are all rare (*59*, *60*), and although there are variants in *ADAM10* known to affect the function or expression of ADAM10, these variants also occur infrequently (*61*). By excluding low frequency and rare variants, this analysis was not able to identify genetic signals in these genes. Additional studies of sequence data in a larger sample size will be necessary to determine the role of *TYROBP*, *ADAM10*, or *ADAM17* in CSF sTREM2 modulation. A second limitation of this study is that we cannot conclude whether other genes in the *MS4A* locus also modulate sTREM2. Our data indicate that *MS4A4A* modulates CSF sTREM2. This is supported by the eQTL analyses, the correlation of *MS4A4A* and *TREM2* mRNA, the identification of a nonsynonymous *MS4A4A* variant associated with CSF sTREM2, and our functional studies. Our preliminary functional studies suggest that MS4A6A does not modify sTREM2, but due to limited availability of MS4A6A reagents, we cannot definitively rule out a relationship between MS4A6A and sTREM2. Given that the GWAS and bioinformatics analyses only consistently supported a putative functional role for *MS4A4A* and *MS4A6A*, we did not investigate the other *MS4A* gene family members; therefore, we cannot exclude the possibility that other genes in the *MS4A* region modulate sTREM2. Another limitation of this study is that we are only beginning to uncover the functional relationship between MS4A4A and sTREM2. The importance of this study resides in the identification and functional validation associating MS4A4A with sTREM2. This study also begins to provide a functional explanation for the original AD risk association identified in the *MS4A* gene region. Our functional data support the genetic association between *MS4A4A* and sTREM2 because we were able to modify extracellular sTREM2 by modulating *MS4A4A* expression or targeting MS4A4A with specific antibodies in human macrophages in vitro. MS4A4A may modify sTREM2 as part of the machinery needed for TREM2 cleavage, through intracellular TREM2 trafficking, or by binding to extracellular sTREM2. Additional functional studies interrogating all of the possible mechanisms by which MS4A4A regulates sTREM2 concentrations will be necessary to address these important questions. In summary, this study identified MS4A4A as an important player in TREM2 biology, provided a mechanistic explanation of the *MS4A* genetic association with AD risk, and demonstrated that sTREM2 may be involved in AD pathology.

MATERIALS AND METHODS

Study design

The goal of this study was to identify common genetic variants and genes associated with CSF sTREM2. To do this, we used a three-stage GWAS: discovery, replication, and meta-analyses. The discovery phase included 813 individuals from the ADNI cohort, and the replication phase included 580 independent CSF samples obtained from AD cases and elderly healthy individuals (Table 1) from six different studies. Meta-analyses were performed using a fixed-effects model. Genetic loci that passed the multiple test correction for GWAS ($P < 5 \times 10^{-8}$) were functionally annotated using bioinformatics tools to identify variants and genes most likely driving the GWAS signal.

To validate the genetic findings, we performed cell-based studies modeling the most likely functional genes identified by the functional annotation. Our analyses identified *MS4A4A* and *MS4A6A* as putative functional genes. Our hypothesis was that changes in concentrations or function of the proteins encoded by these genes should also result in changes in sTREM2. These genes, as well as *TREM2*, are primarily expressed in microglia in the brain. In addition, *MS4A4A* does not have a mouse ortholog. For this reason, we decided to use primary human macrophages cultured in vitro. Transfecting/transducing primary human macrophages is challenging; therefore, we decided to first use antibodies against MS4A4A and MS4A6A as a quick screening method. Primary human macrophages were treated with specific anti-MS4A antibodies, and sTREM2 was measured in the culture medium by ELISA. Then, we transduced primary human macrophages using lentivirus to overexpress *MS4A4A*. ELISA was used to measure sTREM2 in the culture medium.

The Institutional Review Boards of all participating institutions approved the study, and research was carried out in accordance with the approved protocols. Written informed consent was obtained from participants or their family members.

Cohort demographics

CSF was obtained from the ADNI, and sTREM2 was measured with ELISA by a group of investigators at Washington University in St. Louis (WashU) and a group at Ludwig-Maximilians-Universität (LMU) München Department of Neurology (Munich, Germany). A total of 172 AD, 169 cognitive normal, 183 EMCI, 221 late MCI, and 68 SMC individuals were studied in addition to 38 *TREM2* mutation carriers (p.D87N, p.H157Y, p.L211P, p.R47H, and p.R62H). *TREM2* risk-variant carriers were excluded from the GWAS analyses.

Demographic characteristics of the datasets can be seen in Tables 1 and 2 and tables S1 and S3. Additional datasets were used for replication of the top SNPs, and demographic characteristics are shown in table S3. Data were obtained from Knight ADRC, GHPH, GHDEM, SPIN, Clinic-IDIBAPS, and DIAN (*24*–*26*, *32*).

RNA-seq data were obtained from four independent cohorts as described previously (*37*). The Knight ADRC provided data from 28 brains taken from neuropathologically confirmed late-onset AD, an additional 10 AD cases with known *TREM2* mutations, and 14 cognitively healthy controls. DIAN provided data from 19 autosomal dominantly inherited early-onset AD. RNA extraction and sequencing methods were described previously (*37*). RNA-seq data were obtained from the Mayo Clinic Brain Bank via the AMP-AD Knowledge portal (www.synapse.org; synapse ID = 5550404; accessed January 2017), and the RNA extraction and sequencing methods were described previously (*62*). The AMP-AD portal was also used to obtain RNA-seq data from the Mount Sinai Brain Bank (www.synapse.org; synapse ID = 3157743; accessed January 2017), which included data from 1030 samples collected from four brain regions taken from 300 individuals, as described previously (*63*). QC and processing were performed as previously described (*37*).

The RNA extraction and sequencing methods for the Mayo Clinic cohort and the AMP-AD cohort were as described previously (*62*, *63*). For the Knight ADRC participants, parietal lobe tissue was obtained from postmortem brain with informed consent for research use and approval by the Washington University in St. Louis review board. RNA was extracted from frozen brain using TissueLyser LT and RNeasy Mini Kit (Qiagen, Hilden, Germany). RNA integrity number (RIN) and DV200 were measured with RNA 6000 Pico Assay using Bioanalyzer 2100 (Agilent Technologies). The RIN was determined by the software on the Bioanalyzer, taking into account the entire electrophoretic trace of the RNA including the presence or absence of degradation products. The DV200 value was defined as the percentage of nucleotides (nt) >200 nt. The yield of each sample was determined by the Quant-iT RNA Assay (Life Technologies) on the Qubit Fluorometer (Thermo Fisher Scientific). The complementary DNA (cDNA) library was prepared with the TruSeq Stranded Total RNA Sample Prep with Ribo-Zero Gold kit (Illumina) and then sequenced at the McDonnell Genome Institute at Washington University in St. Louis. RNA-seq paired-end reads with a read length of 2 × 150 base pairs were generated using Illumina HiSeq 4000 with a mean coverage of 80 million reads per sample. RIN and DV200 were measured with RNA 6000 Pico Assay using Bioanalyzer 2100 (Agilent Technologies). Fast QC was applied to the RNA-seq data to perform a quality check on various aspects of sequencing quality. Data were aligned to human GRCh37 primary assembly using Star v2.5.2b (*64*), and reads alignment was further evaluated by applying Picard CollectRnaSeqMetrics v2.8.2 (http://broadinstitute.github.io/picard/) to examine reads distribution on the genome. Kallisto v0.42.5 (*65*) was used to determine the read count for each transcript and quantified transcript abundance as transcripts per kilobase per million reads mapped (TPM), using gene annotation of *Homo sapiens* reference genome (GENCODE GRCh38) with the following parameter: -t 10 -b 100. Then, we summed the read counts and TPM of all alternative splicing transcripts of a gene to obtain gene expression levels.

Genotyping and imputation

Samples were genotyped with the Illumina 610 or Omniexpress chip. Stringent QC criteria were applied to each genotyping array separately before combining genotype data. The minimum call rate for SNPs and individuals was 98%, and autosomal SNPs not in Hardy-Weinberg equilibrium ($P < 1 \times 10^{-6}$) were excluded. X chromosome SNPs were analyzed to verify gender identification. Unanticipated duplicates and cryptic relatedness (Pihat ≥ 0.25) among samples were tested by pairwise genome-wide estimates of proportion identity-by-descent, and when a pair of identical or related samples was identified, the sample from Knight ADRC or with a higher number of variants that passed QC was prioritized. EIGENSTRAT (*66*) was used to calculate principal components. *APOE* ε2, ε3, and ε4 isoforms were determined by genotyping rs7412 and rs429358 using TaqMan genotyping technology as previously described (*67*–*69*). The 1000 Genomes Project Phase 3 data (October 2014), SHAPEIT v2.r837 (*70*), and IMPUTE2 v2.3.2 (*71*) were used for phasing and imputation. Individual genotypes imputed with a probability of <0.90 were set to missing, and imputed genotypes with a probability of ≥0.90 were analyzed as fully observed. Genotyped and imputed variants with MAF < 0.02 or IMPUTE2 information score < 0.30 were excluded, leaving 7,320,475 variants for analyses.

ELISA for sTREM2 in CSF and cell culture media

CSF samples were obtained and measured separately by investigators at WashU as described previously (*24*) and LMU. CSF sTREM2 measurements from LMU were obtained using an ELISA based on the MSD (meso scale discovery) platform and is comprehensively described in previous publications (*13*, *25*, *26*). The sTREM2 ELISA performed at WashU was developed in-house as described previously (*24*) with some modifications. Briefly, an anti-human TREM2 monoclonal antibody (R&D Systems, catalog no. MAB1828, clone 263602; 0.5 mg/ml) was used as a capture antibody and coated overnight at 4°C on MaxiSorp 96-well plates (Nalge Nunc International, Rochester, NY) in sodium bicarbonate coating buffer [0.015 M Na_2CO_3 and 0.035 M $NaHCO_3$ (pH 9.6)]. After washing, wells were blocked for 4 hours at 37°C with phosphate-buffered saline (PBS)/10% fetal bovine serum (FBS). Freshly thawed CSF and recombinant human TREM2 standard (SinoBiological, catalog no. 11084-H08H-50) were incubated in duplicate overnight at 4°C. For detection, a goat anti-human TREM2 biotinylated polyclonal antibody (R&D Systems, catalog no. BAF1828; 0.2 mg/ml) was diluted in assay buffer (PBS/10% FBS at 1:3000) and incubated for 1.25 hours at room temperature (RT) on an orbital shaker. After washing, wells were incubated with horseradish peroxidase–labeled streptavidin (BD Biosciences, San Jose, CA; diluted 1:3000) for 1 hour at RT with orbital shaking. Horseradish peroxidase visualization was performed with 3,3′,5,5′ tetramethylbenzidine (Sigma-Aldrich, St. Louis, MO) added to each well for 10 min at RT in the dark. Color development was stopped by adding an equal volume of 2.5 N H_2SO_4. Optical density of each well was determined at 450 nm. Washes between the different steps were done four times with PBS/0.05% Tween 20 (Sigma-Aldrich). An internal standard, consisting of a single batch of human CSF positive for sTREM-2, was run in all the assays. Samples were run in duplicate in each assay. Raw values are provided as picograms per milliliter. Inter-assay variability was calculated from duplicate internal standards across 27 plates [coefficient of variation (CV) = 24.01], and intra-assay variability from duplicate measurements was <9.5%.

Measured CSF values were corrected by plate-specific correction factors obtained by each group, and the corrected values were used for analyses. Pearson's correlation was used to compare the corrected sTREM2 values between the two different ELISA methods in overlapping

samples ($n = 980$, $r = 0.834$, $P = 2.2 \times 10^{-254}$). When more than one experiment was performed in vitro to measure sTREM2 in cell culture media, results are expressed as normalized values on untreated controls.

Human macrophage cultures

Peripheral blood mononuclear cells (PBMCs) were purified from human blood on Ficoll-Paque PLUS density gradient (Amersham Biosciences, Piscataway, NJ). To generate macrophages, PBMCs were cultured in six-well culture plates (3×10^6 cell per well) in RPMI 1640 without FBS. After 2 hours of culture, PBMCs were washed twice with 1× PBS and cultured in RPMI supplemented with macrophage colony-stimulating factor (MCSF) (50 ng/ml) for 7 days at 37°C with 5% CO_2. Supernatants from macrophage cultures were collected at different time points, centrifuged at 21,000*g* for 15 min, and filtered through a 0.22-μm filter to remove all cells and membrane debris. Macrophage supernatants were then frozen in aliquots at −80°C until used in the ELISA for human sTREM2.

In vitro experiments with anti-MS4A antibodies

Human macrophages after 7 days in culture were incubated with anti-MS4A4A (10, 5, and 1 μg/ml; BioLegend, catalog no. 372502, clone 5C12) or anti-MS4A6A (10, 5, and 1 μg/ml; Invitrogen, catalog no. PA5-72732) antibodies in the presence or absence of IL-4 (15 ng/ml; PeproTech) in culture. Mouse IgG isotype (Thermo Fisher Scientific, catalog no.10400C) was used as control. After 48 hours, cell culture media were collected, centrifuged at 21,000*g* for 15 min, and filtered through a 0.22-μm filter to remove all cells and membrane debris. Macrophage supernatants were then frozen in aliquots at −80°C until used in the ELISA for human sTREM2.

Lentivirus vector preparation and experiments

Lentiviral vectors encoding human MS4A4A WT cDNA (NM_148975) Myc-DDK-tagged (RC204646L1), GFP (PS100071), the shRNA for MS4A4A (pGFP-C-shLenti MS4A4A (TL303135B), and the control shRNA pGFP-C-shLenti Scrambled (TR30021) were obtained from OriGene and produced as previously described (*72*, *73*). All constructs were verified by Sanger sequencing. To generate viral particles, human embryonic kidney (HEK)–293T cells were transfected using calcium phosphate with the packaging construct and packaging plasmids Gag-Pol, Rev, and VSV-G. Supernatant containing lentiviral particles was collected at 48 and 72 hours after transfection. Viral supernatant was collected according to previously published protocols (*73*). Transduction was carried out with different volumes (1, 5, 10, 50, 100, and 500 μl) of supernatant in HEK-293T cells for 24 hours. Transduction efficiency, defined as percentage of transduced cells expressing GFP, was assessed qualitatively using an Olympus IX81 fluorescence microscope (Center Valley, PA).

Cultured monocyte-derived macrophages were transduced with lentiviral vectors. The highest transduction efficiency (60 to 70%) was reached with 400 μl of unconcentrated virus after 5 days in culture. Macrophages were transduced with lentivirus vector for 24 hours and rinsed, and fresh media were added. Cells and media were collected 48 hours later for sTREM2 ELISA and quantitative polymerase chain reaction (qPCR) analyses.

Monocyte-derived macrophages were transduced with lentiviral particles to knock down *MS4A4A* [pGFP-C-shLenti MS4A4A (OriGene: TL303135B)] or a control shRNA [pGFP-C-shLenti Scrambled (OriGene: TR30021)]. Macrophages were transduced with lentiviral particles for 48 hours. At day 7, cells were detached and fluorescence-activated cell–sorted for GFP-positive populations using Becton Dickinson FACSAria II cell sorter. GFP-positive sorted cells were replated, and media and cell pellets were collected 3 days later for sTREM2 ELISA and qPCR analyses.

Quantitative PCR

The effect of overexpression was measured by real-time qPCR analysis using probes specific for *MS4A4A*. Macrophages transduced with the lentiviral particles were collected in TRIzol reagent, and total RNA was extracted using the RNeasy Mini Kit (Qiagen). cDNA was prepared from the total RNA using the High-Capacity cDNA Reverse Transcription Kit (Thermo Fisher Scientific). Gene expression levels were analyzed by real-time PCR using TaqMan assays for *MS4A4A* (Hs00254780_m1) and *GAPDH* (Hs02758991_g1) on the QuantStudio 12K Flex Real-Time PCR System (Thermo Fisher Scientific). To avoid amplification interference, expression assays were run in separate wells from the housekeeping gene *GAPDH*. Real-time data were analyzed by the comparative C_T method. Average C_T values for each sample were normalized to the average C_T values for the housekeeping gene *GAPDH*. The resulting value was corrected for assay efficiency. Samples with an SE of 20% or less were analyzed.

Immunocytochemistry and cell imaging

Cells were fixed for 15 to 20 min at RT in 4% (w/v) paraformaldehyde (PFA), 4% (w/v) sucrose, 20 mM NaOH, and 5 mM $MgCl_2$ in PBS (pH 7.4). For intracellular staining, cells were permeabilized and blocked for 60 min at RT in 5% horse serum and 0.1% saponin in PBS and incubated at 4°C overnight with human anti-TREM2 (R&D Systems, catalog no. AF1828) and human anti-MS4A4A (BioLegend, clone 5C12) primary antibodies diluted in PBS and 5% horse serum. Samples were analyzed with an Olympus FV1200 scanning confocal microscope and a Zeiss LSM880 laser scanning confocal microscope (Carl Zeiss Inc., Thornwood, NY) equipped with 63×, 1.4 numerical aperture (NA) Zeiss Plan Apochromat oil objective. The Olympus FV1200 laser scanning confocal microscope (Olympus-America Inc., Waltham, MA) was equipped with five detectors: two spectral and one filter-based and two gallium arsenide phosphide (GaAsP) photo-multiplier tubes (PMTs). Images were captured using an Olympus PlanApoN 60×, 1.4 NA super corrected oil objective. The 405-, 488-, and 559-nm diode lasers and 635-nm HeNe (helium neon) lasers were used with an optimal pinhole of 1 airy unit to acquire images. Images were finally processed with ImageJ software. DF ZEN 2.1 black edition software was used to obtain *Z*-stacks through the entire height of the cells with confocal *Z*-slices of 1.5 μm (63×) and an interval of 0.5 μm. Some of the images were acquired using a Nikon Eclipse 90i fluorescent and bright-field microscope and analyzed for quantitation with the MetaMorph 7.7 software.

Statistical methods

Statistical analyses and data visualization were performed in R v3.4.0 (*74*), PLINK v1.9 (*75*), and LocusZoom v1.3 (*76*). Corrected raw values for CSF sTREM2 concentrations were normally distributed, so two-sample *t* tests were used to compare CSF concentrations between males and females. Kruskal-Wallis with post hoc Dunn's test was used for multiple-group comparisons of the *TREM2* mutation carriers and noncarriers. Pearson's product moment correlation coefficient was used for correlation analyses. Single-variant associations with CSF sTREM2 concentrations were tested using the additive linear regression model in PLINK v1.9 (*75*). Covariates included age at

time of lumbar puncture, sex, and the first two principal component factors to account for population structure. To determine whether there were spurious associations due to differences in the assay, we tested the CSF sTREM2 measurements from WashU and LMU, and in both cases, a genome-wide signal in the *MS4A* cluster was found (Fig. 1 and fig. S3). The genomic inflation factor was $\lambda < 1.008$ for all of the genetic analyses. Statistical significance for single-variant analyses was selected based on the commonly used threshold estimated from Bonferroni correction of the likely number of independent tests in genome-wide analyses ($P < 5 \times 10^{-8}$). Meta-analyses were performed using a fixed effect model in METAL (*77*).

To identify additional independent genetic signals, conditional analyses were conducted by adding the SNP with the smallest *P* value as a covariate into the default regression model and testing all remaining regional SNPs for association. The dataset was stratified by the most recently reported case status, and the genetic signals from the joint dataset were tested to determine whether the genetic associations were driven by cases or controls. To determine whether the identified genetic association within the joint dataset was sex specific, the dataset was stratified by sex and each sex was tested for the association. Results from the sex-specific analyses were verified in a subset of age-matched samples ($n = 367$ each for males and females; table S1).

Gene expression was inferred using Salmon v0.7.2 (*78*) transcript expression quantification of the coding transcripts of *H. sapiens* included in the GENCODE reference genome (GRCh37.75). Gene counts data were transformed to stabilize expression variances along the range of mean values and normalized according to library size using the variance-stabilizing transformation (VST) function in DESeq2 (*79*). Correlations between expression of *TREM2* and each member of the *MS4A* gene family, with an average TPM > 1, were tested in each independent RNA-seq cohort. Differences in mRNA expression and sTREM2 production for the cell-based studies were analyzed using the nonparametric Mann-Whitney test or Kruskal-Wallis *H* test for multigroup comparisons.

Mendelian randomization

We used the R package MendelianRandomization (*80*), which includes three primary methods: inverse-variance weighted, median-based (simple or weighted), and MR-Egger. The MR-Egger method has an option to use robust regression instead of standard regression or a penalized option that downweights the contribution of genetic variants with outlying (heterogeneous) causal estimates. We tested all three primary methods and the different options for the MR-Egger method.

The SNPs selected for the analysis were the two independent SNPs (rs1582763 and rs659156) from chromosome 11 and the top SNP in chromosome 6 (rs28385608). This SNP was included because the locus was near significant in the gene-based analyses, and this SNP had the smallest *P* value within the region in the single-variant analysis. The beta-coefficients and SEs for the three selected SNPs from this study were used as input with summary statistics from a large GWAS for AD risk (*36*).

Bioinformatics annotation

All variants below the threshold for suggestive significance ($P < 1 \times 10^{-5}$) were taken forward for functional annotation using ANNOVAR version 2015-06-17 (*81*) and examined for potential regulatory functions using HaploReg v4.1 (*82*) and RegulomeDB v1.1 (*83*). Search tools from publicly available databases, GTEx Analysis V7 (*84*), the Braineac (*85*), and the Westra Blood eQTL browser (*48*), were used to determine whether significant SNPs were reported eQTLs. The Encyclopedia of DNA elements (ENCODE; www.encodeproject.org/) was queried, filtering for brain tissue in *H. sapiens*, to examine DNA elements affected by the associated SNPs. The Ensembl Variant Effect Predictor (VEP; http://grch37.ensembl.org/Homo_sapiens/Tools/VEP) (*86*) was queried for the predicted effects of identified coding variants, including any applicable SIFT and PolyPhen scores.

SUPPLEMENTARY MATERIALS

stm.sciencemag.org/cgi/content/full/11/505/eaau2291/DC1

Fig. S1. CSF sTREM2 is highly correlated with age and CSF tau.
Fig. S2. CSF sTREM2 concentration is higher in carriers of *TREM2* p.R47H than elderly nondemented individuals.
Fig. S3. The *MS4A* gene region is associated with CSF sTREM2 in a GWAS.
Fig. S4. The association of *MS4A* with sTREM2 is driven by both AD cases and controls.
Fig. S5. No common variants that pass multiple test correction were found to be associated with sTREM2 in the *ADAM17*, *ADAM10*, *TREM2*, or *APOE* gene regions.
Fig. S6. *TREM2*, *MS4A4A*, *MS4A6A*, and *MS4A7* brain mRNAs are highly correlated in AD cases and controls.
Fig. S7. The correlation of *TREM2*, *MS4A4A*, *MS4A6A*, and *MS4A7* brain mRNA replicates in independent cohorts.
Fig. S8. The correlation of *TREM2*, *MS4A4A*, *MS4A6A*, and MS4A7 brain mRNA is found in multiple cortical areas.
Fig. S9. Cell-based studies indicate that MS4A4A, but not MS4A6A, regulates sTREM2 concentrations.
Fig. S10. Silencing of *MS4A4A* leads to a decrease in sTREM2.
Table S1. ADNI CSF cohort characteristics.
Table S2. Functional annotation for all variants with a suggestive association ($P < 1 \times 10^{-5}$) with CSF sTREM2.
Table S3. Epidemiological characteristics for the replication datasets.
Table S4. Results from individual single-variant analyses of replication datasets for rs1582763 and rs6591561.
Table S5. Braineac cis-eQTL results for rs6591561 (uncorrected $P < 0.001$) in average all regions (aveALL), frontal cortex (FCTX), hippocampus (HIPP), and temporal cortex (TCTX).
Table S6. Braineac cis-eQTL results for rs1582763 (uncorrected $P < 0.001$) in average all regions (aveALL), frontal cortex (FCTX), hippocampus (HIPP), and temporal cortex (TCTX).
Table S7. Gene expression correlation results from Knight ADRC and DIAN RNA-seq analyses, testing *TREM2* expression against *MS4A4A* or *MS4A6A*.
Table S8. Gene expression correlation results from Mayo RNA-seq analyses from temporal cortex, testing *TREM2* expression against *MS4A4A* or *MS4A6A*.
Table S9. Gene expression correlation results from Mount Sinai Brain Bank RNA-seq analyses from Brodmann areas 36 or 44, testing TREM2 expression against MS4A4A or MS4A6A.
Data file S1. Individual-level data for Fig. 5 and figs. S9 and S10.

REFERENCES AND NOTES

1. R. Guerreiro, A. Wojtas, J. Bras, M. Carrasquillo, E. Rogaeva, E. Majounie, C. Cruchaga, C. Sassi, J. S. Kauwe, S. Younkin, L. Hazrati, J. Collinge, J. Pocock, T. Lashley, J. Williams, J. C. Lambert, P. Amouyel, A. Goate, R. Rademakers, K. Morgan, J. Powell, P. St. George-Hyslop, A. Singleton, J. Hardy; Alzheimer Genetic Analysis Group, TREM2 variants in Alzheimer's disease. *N. Engl. J. Med.* **368**, 117–127 (2013).
2. T. Jonsson, H. Stefansson, S. Steinberg, I. Jonsdottir, P. V. Jonsson, J. Snaedal, S. Bjornsson, J. Huttenlocher, A. I. Levey, J. J. Lah, D. Rujescu, H. Hampel, I. Giegling, O. A. Andreassen, K. Engedal, I. Ulstein, S. Djurovic, C. Ibrahim-Verbaas, A. Hofman, M. A. Ikram, C. M. van Duijn, U. Thorsteinsdottir, A. Kong, K. Stefansson, Variant of TREM2 associated with the risk of Alzheimer's disease. *N. Engl. J. Med.* **368**, 107–116 (2013).
3. E. O. Luis, S. Ortega-Cubero, I. Lamet, C. Razquin, C. Cruchaga, B. A. Benitez, E. Lorenzo, J. Irigoyen; Alzheimer's Disease Neuroimaging Initiative (ADNI), M. A. Pastor, P. Pastor, Frontobasal gray matter loss is associated with the *TREM2* p.R47H variant. *Neurobiol. Aging* **35**, 2681–2690 (2014).
4. R. Guerreiro, B. Bilgic, G. Guven, J. Brás, J. Rohrer, E. Lohmann, H. Hanagasi, H. Gurvit, M. Emre, A novel compound heterozygous mutation in *TREM2* found in a Turkish frontotemporal dementia-like family. *Neurobiol. Aging* **34**, 2890.e1–2890.e5 (2013).
5. B. A. Benitez, B. Cooper, P. Pastor, S.-C. Jin, E. Lorenzo, S. Cervantes, C. Cruchaga, *TREM2* is associated with the risk of Alzheimer's disease in Spanish population. *Neurobiol. Aging* **34**, 1711.e15–1717.e17 (2013).
6. S. C. Jin, B. A. Benitez, C. M. Karch, B. Cooper, T. Skorupa, D. Carrell, J. B. Norton, S. Hsu, O. Harari, Y. Cai, S. Bertelsen, A. M. Goate, C. Cruchaga, Coding variants in TREM2 increase risk for Alzheimer's disease. *Hum. Mol. Genet.* **23**, 5838–5846 (2014).

7. S. C. Jin, M. M. Carrasquillo, B. A. Benitez, T. Skorupa, D. Carrell, D. Patel, S. Lincoln, S. Krishnan, M. Kachadoorian, C. Reitz, R. Mayeux, T. S. Wingo, J. J. Lah, A. I. Levey, J. Murrell, H. Hendrie, T. Foroud, N. R. Graff-Radford, A. M. Goate, C. Cruchaga, N. Ertekin-Taner, TREM2 is associated with increased risk for Alzheimer's disease in African Americans. *Mol. Neurodegener.* **10**, 19 (2015).
8. S. E. Hickman, J. El Khoury, TREM2 and the neuroimmunology of Alzheimer's disease. *Biochem. Pharmacol.* **88**, 495–498 (2014).
9. Y. Wang, M. Cella, K. Mallinson, J. D. Ulrich, K. L. Young, M. L. Robinette, S. Gilfillan, G. M. Krishnan, S. Sudhakar, B. H. Zinselmeyer, D. M. Holtzman, J. R. Cirrito, M. Colonna, TREM2 lipid sensing sustains the microglial response in an Alzheimer's disease model. *Cell* **160**, 1061–1071 (2015).
10. J. D. Ulrich, T. K. Ulland, M. Colonna, D. M. Holtzman, Elucidating the role of TREM2 in Alzheimer's disease. *Neuron* **94**, 237–248 (2017).
11. C. Cantoni, B. Bollman, D. Licastro, M. Xie, R. Mikesell, R. Schmidt, C. M. Yuede, D. Galimberti, G. Olivecrona, R. S. Klein, A. H. Cross, K. Otero, L. Piccio, TREM2 regulates microglial cell activation in response to demyelination in vivo. *Acta Neuropathol.* **129**, 429–447 (2015).
12. Y. Deming, Z. Li, B. A. Benitez, C. Cruchaga, Triggering receptor expressed on myeloid cells 2 (TREM2): A potential therapeutic target for Alzheimer disease? *Expert Opin. Ther. Targets* **22**, 587–598 (2018).
13. G. Kleinberger, Y. Yamanishi, M. Suarez-Calvet, E. Czirr, E. Lohmann, E. Cuyvers, H. Struyfs, N. Pettkus, A. Wenninger-Weinzierl, F. Mazaheri, S. Tahirovic, A. Lleó, D. Alcolea, J. Fortea, M. Willem, S. Lammich, J. L. Molinuevo, R. Sanchez-Valle, A. Antonell, A. Ramirez, M. T. Heneka, K. Sleegers, J. van der Zee, J.-J. Martin, S. Engelborghs, A. Demirtas-Tatlidede, H. Zetterberg, C. Van Broeckhoven, H. Gurvit, T. Wyss-Coray, J. Hardy, M. Colonna, C. Haass, TREM2 mutations implicated in neurodegeneration impair cell surface transport and phagocytosis. *Sci. Transl. Med.* **6**, 243ra286 (2014).
14. C. Y. D. Lee, A. Daggett, X. Gu, L. L. Jiang, P. Langfelder, X. Li, N. Wang, Y. Zhao, C. S. Park, Y. Cooper, I. Ferando, I. Mody, G. Coppola, H. Xu, X. W. Yang, Elevated TREM2 gene dosage reprograms microglia responsivity and ameliorates pathological phenotypes in Alzheimer's disease models. *Neuron* **97**, 1032–1048.e5 (2018).
15. J. D. Ulrich, M. B. Finn, Y. Wang, A. Shen, T. E. Mahan, H. Jiang, F. R. Stewart, L. Piccio, M. Colonna, D. M. Holtzman, Altered microglial response to Aβ plaques in APPPS1-21 mice heterozygous for TREM2. *Mol. Neurodegener.* **9**, 20 (2014).
16. Y. Wang, T. K. Ulland, J. D. Ulrich, W. Song, J. A. Tzaferis, J. T. Hole, P. Yuan, T. E. Mahan, Y. Shi, S. Gilfillan, M. Cella, J. Grutzendler, R. B. DeMattos, J. R. Cirrito, D. M. Holtzman, M. Colonna, TREM2-mediated early microglial response limits diffusion and toxicity of amyloid plaques. *J. Exp. Med.* **213**, 667–675 (2016).
17. P. Yuan, C. Condello, C. D. Keene, Y. Wang, T. D. Bird, S. M. Paul, W. Luo, M. Colonna, D. Baddeley, J. Grutzendler, trem2 haplodeficiency in mice and humans impairs the microglia barrier function leading to decreased amyloid compaction and severe axonal dystrophy. *Neuron* **92**, 252–264 (2016).
18. C. E. G. Leyns, J. D. Ulrich, M. B. Finn, F. R. Stewart, L. J. Koscal, J. Remolina Serrano, G. O. Robinson, E. Anderson, M. Colonna, D. M. Holtzman, TREM2 deficiency attenuates neuroinflammation and protects against neurodegeneration in a mouse model of tauopathy. *Proc. Natl. Acad. Sci. U.S.A.* **114**, 11524–11529 (2017).
19. S. M. Bemiller, T. J. McCray, K. Allan, S. V. Formica, G. Xu, G. Wilson, O. N. Kokiko-Cochran, S. D. Crish, C. A. Lasagna-Reeves, R. M. Ransohoff, G. E. Landreth, B. T. Lamb, TREM2 deficiency exacerbates tau pathology through dysregulated kinase signaling in a mouse model of tauopathy. *Mol. Neurodegener.* **12**, 74 (2017).
20. P. Wunderlich, K. Glebov, N. Kemmerling, N. T. Tien, H. Neumann, J. Walter, Sequential proteolytic processing of the triggering receptor expressed on myeloid cells-2 (TREM2) protein by ectodomain shedding and γ-secretase-dependent intramembranous cleavage. *J. Biol. Chem.* **288**, 33027–33036 (2013).
21. K. Schlepckow, G. Kleinberger, A. Fukumori, R. Feederle, S. F. Lichtenthaler, H. Steiner, C. Haass, An Alzheimer-associated TREM2 variant occurs at the ADAM cleavage site and affects shedding and phagocytic function. *EMBO Mol. Med.* **9**, 1356–1365 (2017).
22. P. Thornton, J. Sevalle, M. J. Deery, G. Fraser, Y. Zhou, S. Ståhl, E. H. Franssen, R. B. Dodd, S. Qamar, B. Gomez Perez-Nievas, L. S. C. Nicol, S. Eketjall, J. Revell, C. Jones, A. Billinton, P. H. St George-Hyslop, I. Chessell, D. C. Crowther, TREM2 shedding by cleavage at the H157-S158 bond is accelerated for the Alzheimer's disease-associated H157Y variant. *EMBO Mol. Med.* **9**, 1366–1378 (2017).
23. A. Heslegrave, W. Heywood, R. Paterson, N. Magdalinou, J. Svensson, P. Johansson, A. Öhrfelt, K. Blennow, J. Hardy, J. Schott, K. Mills, H. Zetterberg, Increased cerebrospinal fluid soluble TREM2 concentration in Alzheimer's disease. *Mol. Neurodegener.* **11**, 3 (2016).
24. L. Piccio, Y. Deming, J. L. Del-Águila, L. Ghezzi, D. M. Holtzman, A. M. Fagan, C. Fenoglio, D. Galimberti, B. Borroni, C. Cruchaga, Cerebrospinal fluid soluble TREM2 is higher in Alzheimer disease and associated with mutation status. *Acta Neuropathol.* **131**, 925–933 (2016).
25. M. Suárez-Calvet, M. Á. Araque Caballero, G. Kleinberger, R. J. Bateman, A. M. Fagan, J. C. Morris, J. Levin, A. Danek, M. Ewers, C. Haass; Dominantly Inherited Alzheimer Network, Early changes in CSF sTREM2 in dominantly inherited alzheimer's disease occur after amyloid deposition and neuronal injury. *Sci. Transl. Med.* **8**, 369ra178 (2016).
26. M. Suárez-Calvet, G. Kleinberger, M. Á. Araque Caballero, M. Brendel, A. Rominger, D. Alcolea, J. Fortea, A. Lleó, R. Blesa, J. D. Gispert, R. Sánchez-Valle, A. Antonell, L. Rami, J. L. Molinuevo, F. Brosseron, A. Traschütz, M. T. Heneka, H. Struyfs, S. Engelborghs, K. Sleegers, C. Van Broeckhoven, H. Zetterberg, B. Nellgard, K. Blennow, A. Crispin, M. Ewers, C. Haass, sTREM2 cerebrospinal fluid levels are a potential biomarker for microglia activity in early-stage Alzheimer's disease and associate with neuronal injury markers. *EMBO Mol. Med.* **8**, 466–476 (2016).
27. L. Piccio, C. Buonsanti, M. Cella, I. Tassi, R. E. Schmidt, C. Fenoglio, J. Rinker II, R. T. Naismith, P. Panina-Bordignon, N. Passini, D. Galimberti, E. Scarpini, M. Colonna, A. H. Cross, Identification of soluble TREM-2 in the cerebrospinal fluid and its association with multiple sclerosis and CNS inflammation. *Brain* **131**, 3081–3091 (2008).
28. K. Henjum, I. S. Almdahl, V. Arskog, L. Minthon, O. Hansson, T. Fladby, L. N. Nilsson, Cerebrospinal fluid soluble TREM2 in aging and Alzheimer's disease. *Alzheimers Res. Ther.* **8**, 17 (2016).
29. B. Benyamin, A. F. Mcrae, G. Zhu, S. Gordon, A. K. Henders, A. Palotie, L. Peltonen, N. G. Martin, G. W. Montgomery, J. B. Whitfield, P. M. Visscher, Variants in *TF* and *HFE* explain similar to ~ 40% of genetic variation in serum-transferrin levels. *Am. J. Hum. Genet.* **84**, 60–65 (2009).
30. K. Panoutsopoulou, S. Thiagarajah, A. Day-Williams, L. Southam, K. Hatzikotoulas, A. Matchan, M. Doherty, J. M. Wilkinson, E. Zeggini; arcOGEN Consortium, Powerful detection of osteoarthritis susceptibility loci by comprehensive examination of clinically important endophenotypes. *Osteoarthr. Cartil.* **22**, S232 (2014).
31. Y. Deming, Z. Li, M. Kapoor, O. Harari, J. L. Del-Aguila, K. Black, D. Carrell, Y. Cai, M. V. Fernandez, J. Budde, S. Ma, B. Saef, B. Howells, K.-I. Huang, S. Bertelsen, A. M. Fagan, D. M. Holtzman, J. C. Morris, S. Kim, A. J. Saykin, P. L. De Jager, M. Albert, A. Moghekar, R. O'Brien, M. Riemenschneider, R. C. Petersen, K. Blennow, H. Zetterberg, L. Minthon, V. M. Van Deerlin, V. M.-Y. Lee, L. M. Shaw, J. Q. Trojanowski, G. Schellenberg, J. L. Haines, R. Mayeux, M. A. Pericak-Vance, L. A. Farrer, E. R. Peskind, G. Li, A. F. Di Narzo, Alzheimer's Disease Neuroimaging Initiative (ADNI), Alzheimer Disease Genetic Consortium (ADGC), J. S. K. Kauwe, A. M. Goate, C. Cruchaga, Genome-wide association study identifies four novel loci associated with Alzheimer's endophenotypes and disease modifiers. *Acta Neuropathol.* **133**, 839–856 (2017).
32. P. Johansson, N. Mattsson, O. Hansson, A. Wallin, J. O. Johansson, U. Andreasson, H. Zetterberg, K. Blennow, J. Svensson, Cerebrospinal fluid biomarkers for Alzheimer's disease: Diagnostic performance in a homogeneous mono-center population. *J. Alzheimers Dis.* **24**, 537–546 (2011).
33. K. D. Coon, A. J. Myers, D. W. Craig, J. A. Webster, J. V. Pearson, D. H. Lince, V. L. Zismann, T. G. Beach, D. Leung, L. Bryden, R. F. Halperin, L. Marlowe, M. Kaleem, D. G. Walker, R. Ravid, C. B. Heward, J. Rogers, A. Papassotiropoulos, E. M. Reiman, J. Hardy, D. A. Stephan, A high-density whole-genome association study reveals that APOE is the major susceptibility gene for sporadic late-onset Alzheimer's disease. *J. Clin. Psychiatry* **68**, 613–618 (2007).
34. C. Cruchaga, J. S. K. Kauwe, O. Harari, S. C. Jin, Y. Cai, C. M. Karch, B. A. Benitez, A. T. Jeng, T. Skorupa, D. Carrell, S. Bertelsen, M. Bailey, D. McKean, J. M. Shulman, P. L. De Jager, L. Chibnik, D. A. Bennett, S. E. Arnold, D. Harold, R. Sims, A. Gerrish, J. Williams, V. M. Van Deerlin, V. M.-Y. Lee, L. M. Shaw, J. Q. Trojanowski, J. L. Haines, R. Mayeux, M. A. Pericak-Vance, L. A. Farrer, G. D. Schellenberg, E. R. Peskind, D. Galasko, A. M. Fagan, D. M. Holtzman, J. C. Morris; GERAD Consortium; Alzheimer's Disease Neuroimaging Initiative (ADNI), Alzheimer Disease Genetic Consortium (ADGC), A. M. Goate, GWAS of cerebrospinal fluid tau levels identifies risk variants for Alzheimer's disease. *Neuron* **78**, 256–268 (2013).
35. R. Lautner, S. Palmqvist, N. Mattsson, U. Andreasson, A. Wallin, E. Pålsson, J. Jakobsson, S. K. Herukka, R. Owenius, B. Olsson, H. Hampel, D. Rujescu, M. Ewers, M. Landén, L. Minthon, K. Blennow, H. Zetterberg, O. Hansson; Alzheimer's Disease Neuroimaging Initiative, Disease Neuroimaging, Apolipoprotein E genotype and the diagnostic accuracy of cerebrospinal fluid biomarkers for Alzheimer disease. *JAMA Psychiat.* **71**, 1183–1191 (2014).
36. J.-C. Lambert, C. A. Ibrahim-Verbaas, D. Harold, A. C. Naj, R. Sims, C. Bellenguez, G. Jun, A. L. De Stefano, J. C. Bis, G. W. Beecham, B. Grenier-Boley, G. Russo, T. A. Thornton-Wells, N. Jones, A. V. Smith, V. Chouraki, C. Thomas, M. A. Ikram, D. Zelenika, B. N. Vardarajan, Y. Kamatani, C.-F. Lin, A. Gerrish, H. Schmidt, B. Kunkle, M. L. Dunstan, A. Ruiz, M.-T. Bihoreau, S.-H. Choi, C. Reitz, F. Pasquier, P. Hollingworth, A. Ramirez, O. Hanon, A. L. Fitzpatrick, J. D. Buxbaum, D. Campion, P. K. Crane, C. Baldwin, T. Becker, V. Gudnason, C. Cruchaga, D. Craig, N. Amin, C. Berr, O. L. Lopez, P. L. De Jager, V. Deramecourt, J. A. Johnston, D. Evans, S. Lovestone, L. Letenneur, F. J. Morón, D. C. Rubinsztein, G. Eiriksdottir, K. Sleegers, A. M. Goate, N. Fiévet, M. J. Huentelman, M. Gill, K. Brown, M. I. Kamboh, L. Keller, P. Barberger-Gateau, B. M. Guinness, E. B. Larson, R. Green, A. J. Myers, C. Dufouil, S. Todd, D. Wallon, S. Love, E. Rogaeva, J. Gallacher,

P. St. George-Hyslop, J. Clarimon, A. Lleo, A. Bayer, D. W. Tsuang, L. Yu, M. Tsolaki, P. Bossù, G. Spalletta, P. Proitsi, J. Collinge, S. Sorbi, F. Sanchez-Garcia, N. C. Fox, J. Hardy, M. C. D. Naranjo, P. Bosco, R. Clarke, C. Brayne, D. Galimberti, M. Mancuso, F. Matthews; European Alzheimer's Disease Initiative (EADI), Genetic and Environmental Risk in Alzheimer's Disease (GERAD); Alzheimer's Disease Genetic Consortium (ADGC), Cohorts for Heart and Aging Research in Genomic Epidemiology (CHARGE), S. Moebus, P. Mecocci, M. D. Zompo, W. Maier, H. Hampel, A. Pilotto, M. Bullido, F. Panza, P. Caffarra, B. Nacmias, J. R. Gilbert, M. Mayhaus, L. Lannfelt, H. Hakonarson, S. Pichler, M. M. Carrasquillo, M. Ingelsson, D. Beekly, V. Alvarez, F. Zou, O. Valladares, S. G. Younkin, E. Coto, K. L. Hamilton-Nelson, W. Gu, C. Razquin, P. Pastor, I. Mateo, M. J. Owen, K. M. Faber, P. V. Jonsson, O. Combarros, M. C. O'Donovan, L. B. Cantwell, H. Soininen, D. Blacker, S. Mead, T. H. Mosley Jr., D. A. Bennett, T. B. Harris, L. Fratiglioni, C. Holmes, R. F. A. G. de Bruijn, P. Passmore, T. J. Montine, K. Bettens, J. I. Rotter, A. Brice, K. Morgan, T. M. Foroud, W. A. Kukull, D. Hannequin, J. F. Powell, M. A. Nalls, K. Ritchie, K. L. Lunetta, J. S. K. Kauwe, E. Boerwinkle, M. Riemenschneider, M. Boada, M. Hiltunen, E. R. Martin, R. Schmidt, D. Rujescu, L.-S. Wang, J.-F. Dartigues, R. Mayeux, C. Tzourio, A. Hofman, M. M. Nöthen, C. Graff, B. M. Psaty, L. Jones, J. L. Haines, P. A. Holmans, M. Lathrop, M. A. Pericak-Vance, L. J. Launer, L. A. Farrer, C. M. van Duijn, C. Van Broeckhoven, V. Moskvina, S. Seshadri, J. Williams, G. D. Schellenberg, P. Amouyel, Meta-analysis of 74,046 individuals identifies 11 new susceptibility loci for Alzheimer's disease. *Nat. Genet.* **45**, 1452–1458 (2013).

37. Z. Li, J. L. Del Aguila, U. Dube, J. Budde, R. Martinez, K. Black, Q. Xiao, N. J. Cairns; Dominantly Inherited Alzheimer Network (DIAN), J. D. Dougherty, J.-M. Lee, J. C. Morris, R. J. Bateman, C. M. Karch, C. Cruchaga, O. Harari, Genetic variants associated with Alzheimer's disease confer different cerebral cortex cell-type population structure. *Genome Med.* **10**, (2018).
38. Y. Zhang, K. Chen, S. A. Sloan, M. L. Bennett, A. R. Scholze, S. O'Keeffe, H. P. Phatnani, P. Guarnieri, C. Caneda, N. Ruderisch, S. Deng, S. A. Liddelow, C. Zhang, R. Daneman, T. Maniatis, B. A. Barres, J. Q. Wu, An RNA-sequencing transcriptome and splicing database of glia, neurons, and vascular cells of the cerebral cortex. *J. Neurosci.* **34**, 11929–11947 (2014).
39. Y. Zhang, S. A. Sloan, L. E. Clarke, C. Caneda, C. A. Plaza, P. D. Blumenthal, H. Vogel, G. K. Steinberg, M. S. B. Edwards, G. Li, J. A. Duncan III, S. H. Cheshier, L. M. Shuer, E. F. Chang, G. A. Grant, M. G. Gephart, B. A. Barres, Purification and characterization of progenitor and mature human astrocytes reveals transcriptional and functional differences with mouse. *Neuron* **89**, 37–53 (2016).
40. K.-I. Huang, E. Marcora, A. A. Pimenova, A. F. Di Narzo, M. Kapoor, S. C. Jin, O. Harari, S. Bertelsen, B. P. Fairfax, J. Czajkowski, V. Chouraki, B. Grenier-Boley, C. Bellenguez, Y. Deming, A. M. Kenzie, T. Raj, A. E. Renton, J. Budde, A. Smith, A. Fitzpatrick, J. C. Bis, A. De Stefano, H. H. H. Adams, M. A. Ikram, S. van der Lee, J. L. Del-Aguila, M. V. Fernandez, L. Ibañez; International Genomics of Alzheimer's Project; Alzheimer's Disease Neuroimaging Initiative, R. Sims, V. Escott-Price, R. Mayeux, J. L. Haines, L. A. Farrer, M. A. Pericak-Vance, J. C. Lambert, C. van Duijn, L. Launer, S. Seshadri, J. Williams, P. Amouyel, G. D. Schellenberg, B. Zhang, I. Borecki, J. S. K. Kauwe, C. Cruchaga, K. Hao, A. M. Goate, A common haplotype lowers PU.1 expression in myeloid cells and delays onset of Alzheimer's disease. *Nat. Neurosci.* **20**, 1052–1061 (2017).
41. M. Cella, C. Buonsanti, C. Strader, T. Kondo, A. Salmaggi, M. Colonna, Impaired differentiation of osteoclasts in TREM-2-deficient individuals. *J. Exp. Med.* **198**, 645–651 (2003).
42. R. Sanyal, M. J. Polyak, J. Zuccolo, M. Puri, L. Deng, L. Roberts, A. Zuba, J. Storek, J. M. Luider, E. M. Sundberg, A. Mansoor, E. Baigorri, M. P. Chu, A. R. Belch, L. M. Pilarski, J. P. Deans, MS4A4A: A novel cell surface marker for M2 macrophages and plasma cells. *Immunol. Cell Biol.* **95**, 611–619 (2017).
43. I. R. Turnbull, S. Gilfillan, M. Cella, T. Aoshi, M. Miller, L. Piccio, M. Hernandez, M. Colonna, Cutting edge: TREM-2 attenuates macrophage activation. *J. Immunol.* **177**, 3520–3524 (2006).
44. G. Cruse, M. A. Beaven, S. C. Music, P. Bradding, A. M. Gilfillan, D. D. Metcalfe, The CD20 homologue MS4A4 directs trafficking of KIT toward clathrin-independent endocytosis pathways and thus regulates receptor signaling and recycling. *Mol. Biol. Cell* **26**, 1711–1727 (2015).
45. S. Carmona, K. Zahs, E. Wu, K. Dakin, J. Bras, R. Guerreiro, The role of *TREM2* in Alzheimer's disease and other neurodegenerative disorders. *Lancet Neurol.* **17**, 721–730 (2018).
46. Y. Deming, J. Xia, Y. F. Cai, J. Lord, J. L. Del-Aguila, M. V. Fernandez, D. Carrell, K. Black, J. Budde, S. Ma, B. Saef, B. Howells, S. Bertelsen, M. Bailey, P. G. Ridge, D. Holtzman; Alzheimer's Disease Neuroimaging Initiative (ADNI), J. C. Morris, K. Bales, E. H. Pickering, J.-M. Lee, L. Heitsch, J. Kauwe, A. Goate, L. Piccio, C. Cruchaga, Adni, Genetic studies of plasma analytes identify novel potential biomarkers for several complex traits. *Sci. Rep.* **6**, 18092 (2016).
47. N. Garge, H. Pan, M. D. Rowland, B. J. Cargile, X. X. Zhang, P. C. Cooley, G. P. Page, M. K. Bunger, Identification of quantitative trait loci underlying proteome variation in human lymphoblastoid cells. *Mol. Cell. Proteomics* **9**, 1383–1399 (2010).
48. H.-J. Westra, M. J. Peters, T. Esko, H. Yaghootkar, C. Schurmann, J. Kettunen, M. W. Christiansen, B. P. Fairfax, K. Schramm, J. E. Powell, A. Zhernakova, D. V. Zhernakova, J. H. Veldink, L. H. Van den Berg, J. Karjalainen, S. Withoff, A. G. Uitterlinden, A. Hofman, F. Rivadeneira, P. A. C. t Hoen, E. Reinmaa, K. Fischer, M. Nelis, L. Milani, D. Melzer, L. Ferrucci, A. B. Singleton, D. G. Hernandez, M. A. Nalls, G. Homuth, M. Nauck, D. Radke, U. Völker, M. Perola, V. Salomaa, J. Brody, A. Suchy-Dicey, S. A. Gharib, D. A. Enquobahrie, T. Lumley, G. W. Montgomery, S. Makino, H. Prokisch, C. Herder, M. Roden, H. Grallert, T. Meitinger, K. Strauch, Y. Li, R. C. Jansen, P. M. Visscher, J. C. Knight, B. M. Psaty, S. Ripatti, A. Teumer, T. M. Frayling, A. Metspalu, J. B. J. van Meurs, L. Franke, Systematic identification of *trans* eQTLs as putative drivers of known disease associations. *Nat. Genet.* **45**, 1238–1243 (2013).
49. K. Suhre, M. Arnold, A. M. Bhagwat, R. J. Cotton, R. Engelke, J. Raffler, H. Sarwath, G. Thareja, A. Wahl, R. K. DeLisle, L. Gold, M. Pezer, G. Lauc, M. A. El-Din Selim, D. O. Mook-Kanamori, E. K. Al-Dous, Y. A. Mohamoud, J. Malek, K. Strauch, H. Grallert, A. Peters, G. Kastenmuller, C. Gieger, J. Graumann, Connecting genetic risk to disease end points through the human blood plasma proteome. *Nat. Commun.* **8**, 14357 (2017).
50. L. Folkersen, E. Fauman, M. Sabater-Lleal, R. J. Strawbridge, M. Franberg, B. Sennblad, D. Baldassarre, F. Veglia, S. E. Humphries, R. Rauramaa, U. de Faire, A. J. Smit, P. Giral, S. Kurl, E. Mannarino, S. Enroth, A. Johansson, S. B. Enroth, S. Gustafsson, L. Lind, C. Lindgren, A. P. Morris, V. Giedraitis, A. Silveira, A. Franco-Cereceda, E. Tremoli, I. s. group, U. Gyllensten, E. Ingelsson, S. Brunak, P. Eriksson, D. Ziemek, A. Hamsten, A. Mälarstig, Mapping of 79 loci for 83 plasma protein biomarkers in cardiovascular disease. *PLOS Genet.* **13**, e1006706 (2017).
51. T.-T. Chang, J.-W. Chen, Emerging role of chemokine CC motif ligand 4 related mechanisms in diabetes mellitus and cardiovascular disease: Friends or foes? *Cardiovasc. Diabetol.* **15**, 117 (2016).
52. T. R. Jay, C. M. Miller, P. J. Cheng, L. C. Graham, S. Bemiller, M. L. Broihier, G. Xu, D. Margevicius, J. C. Karlo, G. L. Sousa, A. C. Cotleur, O. Butovsky, L. Bekris, S. M. Staugaitis, J. B. Leverenz, S. W. Pimplikar, G. E. Landreth, G. R. Howell, R. M. Ransohoff, B. T. Lamb, TREM2 deficiency eliminates TREM2^{+} inflammatory macrophages and ameliorates pathology in Alzheimer's disease mouse models. *J. Exp. Med.* **212**, 287–295 (2015).
53. D. L. Kober, T. J. Brett, TREM2-ligand interactions in health and disease. *J. Mol. Biol.* **429**, 1607–1629 (2017).
54. M. M. Painter, Y. Atagi, C. C. Liu, R. Rademakers, H. Xu, J. D. Fryer, G. Bu, TREM2 in CNS homeostasis and neurodegenerative disease. *Mol. Neurodegener.* **10**, 43 (2015).
55. L. Zhong, X.-F. Chen, T. Wang, Z. Wang, C. Liao, Z. Wang, R. Huang, D. Wang, X. Li, L. Wu, L. Jia, H. Zheng, M. Painter, Y. Atagi, C.-C. Liu, Y.-W. Zhang, J. D. Fryer, H. Xu, G. Bu, Soluble TREM2 induces inflammatory responses and enhances microglial survival. *J. Exp. Med.* **214**, 597–607 (2017).
56. C. E. G. Leyns, D. M. Holtzman, Glial contributions to neurodegeneration in tauopathies. *Mol. Neurodegener.* **12**, 50 (2017).
57. D. I. Swerdlow, K. B. Kuchenbaecker, S. Shah, R. Sofat, M. V. Holmes, J. White, J. S. Mindell, M. Kivimaki, E. J. Brunner, J. C. Whittaker, J. P. Casas, A. D. Hingorani, Selecting instruments for Mendelian randomization in the wake of genome-wide association studies. *Int. J. Epidemiol.* **45**, 1600–1616 (2016).
58. S. Krasemann, C. Madore, R. Cialic, C. Baufeld, N. Calcagno, R. E. Fatimy, L. Beckers, E. O'Loughlin, Y. Xu, Z. Fanek, D. J. Greco, S. T. Smith, G. Tweet, Z. Humulock, T. Zrzavy, P. Conde-Sanroman, M. Gacias, Z. Weng, H. Chen, E. Tjon, F. Mazaheri, K. Hartmann, A. Madi, J. D. Ulrich, M. Glatzel, A. Worthmann, J. Heeren, B. Budnik, C. Lemere, T. Ikezu, F. L. Heppner, V. Litvak, D. M. Holtzman, H. Lassmann, H. L. Weiner, J. Ochando, C. Haass, O. Butovsky, The TREM2-APOE pathway drives the transcriptional phenotype of dysfunctional microglia in neurodegenerative diseases. *Immunity* **47**, 566–581.e9 (2017).
59. J. Paloneva, M. Kestilä, J. Wu, A. Salminen, T. Böhling, V. Ruotsalainen, P. Hakola, A. B. H. Bakker, J. H. Phillips, P. Pekkarinen, L. L. Lanier, T. Timonen, L. Peltonen, Loss-of-function mutations in *TYROBP* (*DAP12*) result in a presenile dementia with bone cysts. *Nat. Genet.* **25**, 357–361 (2000).
60. J. Paloneva, T. Manninen, G. Christman, K. Hovanes, J. Mandelin, R. Adolfsson, M. Bianchin, T. Bird, R. Miranda, A. Salmaggi, L. Tranebjaerg, Y. Konttinen, L. Peltonen, Mutations in two genes encoding different subunits of a receptor signaling complex result in an identical disease phenotype. *Am. J. Hum. Genet.* **71**, 656–662 (2002).
61. L. Cui, Y. Gao, Y. Xie, Y. Wang, Y. Cai, X. Shao, X. Ma, Y. Li, G. Ma, G. Liu, W. Cheng, Y. Liu, T. Liu, Q. Pan, H. Tao, Z. Liu, B. Zhao, Y. Shao, K. Li, An ADAM10 promoter polymorphism is a functional variant in severe sepsis patients and confers susceptibility to the development of sepsis. *Crit. Care* **19**, 73 (2015).
62. M. Allen, M. M. Carrasquillo, C. Funk, B. D. Heavner, F. Zou, C. S. Younkin, J. D. Burgess, H.-S. Chai, J. Crook, J. A. Eddy, H. Li, B. Logsdon, M. A. Peters, K. K. Dang, X. Wang, D. Serie, C. Wang, T. Nguyen, S. Lincoln, K. Malphrus, G. Bisceglio, M. Li, T. E. Golde, L. M. Mangravite, Y. Asmann, N. D. Price, R. C. Petersen, N. R. Graff-Radford, D. W. Dickson, S. G. Younkin, N. Ertekin-Taner, Human whole genome genotype and transcriptome data for Alzheimer's and other neurodegenerative diseases. *Sci. Data* **3**, 160089 (2016).
63. M. Wang, P. Roussos, A. McKenzie, X. Zhou, Y. Kajiwara, K. J. Brennand, G. C. De Luca, J. F. Crary, P. Casaccia, J. D. Buxbaum, M. Ehrlich, S. Gandy, A. Goate, P. Katsel, E. Schadt, V. Haroutunian, B. Zhang, Integrative network analysis of nineteen brain regions

identifies molecular signatures and networks underlying selective regional vulnerability to Alzheimer's disease. *Genome Med.* **8**, 104 (2016).
64. A. Dobin, C. A. Davis, F. Schlesinger, J. Drenkow, C. Zaleski, S. Jha, P. Batut, M. Chaisson, T. R. Gingeras, STAR: Ultrafast universal RNA-seq aligner. *Bioinformatics* **29**, 15–21 (2013).
65. N. L. Bray, H. Pimentel, P. Melsted, L. Pachter, Near-optimal probabilistic RNA-seq quantification. *Nat. Biotechnol.* **34**, 525–527 (2016).
66. A. L. Price, N. J. Patterson, R. M. Plenge, M. E. Weinblatt, N. A. Shadick, D. Reich, Principal components analysis corrects for stratification in genome-wide association studies. *Nat. Genet.* **38**, 904–909 (2006).
67. C. Cruchaga, J. S. K. Kauwe, K. Mayo, N. Spiegel, S. Bertelsen, P. Nowotny, A. R. Shah, R. Abraham, P. Hollingworth, D. Harold, M. M. Owen, J. Williams, S. Lovestone, E. R. Peskind, G. Li, J. B. Leverenz, D. Galasko; Alzheimer's Disease Neuroimaging Initiative, J. C. Morris, A. M. Fagan, D. M. Holtzman, A. M. Goate, SNPs associated with cerebrospinal fluid phospho-tau levels influence rate of decline in Alzheimer's disease. *PLOS Genet.* **6**, e1001101 (2010).
68. C. Cruchaga, J. S. K. Kauwe, P. Nowotny, K. Bales, E. H. Pickering, K. Mayo, S. Bertelsen, A. Hinrichs; Alzheimer's Disease Neuroimaging Initiatives, A. M. Fagan, D. M. Holtzman, J. C. Morris, A. M. Goate, Cerebrospinal fluid APOE levels: An endophenotype for genetic studies for Alzheimer's disease. *Hum. Mol. Genet.* **21**, 4558–4571 (2012).
69. J. S. Kauwe, C. Cruchaga, S. Bertelsen, K. Mayo, W. Latu, P. Nowotny, A. L. Hinrichs, A. M. Fagan, D. M. Holtzman; Alzheimer's Disease Neuroimaging Initiative, A. M. Goate, Validating predicted biological effects of Alzheimer's disease associated SNPs using CSF biomarker levels. *J. Alzheimers Dis.* **21**, 833–842 (2010).
70. O. Delaneau, J. Marchini; The 1000 Genomes Project Consortium, Integrating sequence and array data to create an improved 1000 Genomes Project haplotype reference panel. *Nat. Commun.* **5**, 3934 (2014).
71. B. Howie, C. Fuchsberger, M. Stephens, J. Marchini, G. R. Abecasis, Fast and accurate genotype imputation in genome-wide association studies through pre-phasing. *Nat. Genet.* **44**, 955–959 (2012).
72. T. Dull, R. Zufferey, M. Kelly, R. J. Mandel, M. Nguyen, D. Trono, L. Naldini, A third-generation lentivirus vector with a conditional packaging system. *J. Virol.* **72**, 8463–8471 (1998).
73. B. A. Benitez, M. S. Sands, Primary fibroblasts from CSPalpha mutation carriers recapitulate hallmarks of the adult onset neuronal ceroid lipofuscinosis. *Sci. Rep.* **7**, 6332 (2017).
74. R Core Team (R Foundation for Statistical Computing, Vienna, Austria, 2017).
75. C. C. Chang, C. C. Chow, L. C. A. M. Tellier, S. Vattikuti, S. M. Purcell, J. J. Lee, Second-generation PLINK: Rising to the challenge of larger and richer datasets. *Gigascience* **4**, 7 (2015).
76. R. J. Pruim, R. P. Welch, S. Sanna, T. M. Teslovich, P. S. Chines, T. P. Gliedt, M. Boehnke, G. R. Abecasis, C. J. Willer, LocusZoom: Regional visualization of genome-wide association scan results. *Bioinformatics* **26**, 2336–2337 (2010).
77. C. J. Willer, Y. Li, G. R. Abecasis, METAL: Fast and efficient meta-analysis of genomewide association scans. *Bioinformatics* **26**, 2190–2191 (2010).
78. R. Patro, G. Duggal, M. I. Love, R. A. Irizarry, C. Kingsford, Salmon provides fast and bias-aware quantification of transcript expression. *Nat. Methods* **14**, 417–419 (2017).
79. M. I. Love, W. Huber, S. Anders, Moderated estimation of fold change and dispersion for RNA-seq data with DESeq2. *Genome Biol.* **15**, 550 (2014).
80. O. O. Yavorska, S. Burgess, MendelianRandomization: An R package for performing Mendelian randomization analyses using summarized data. *Int. J. Epidemiol.* **46**, 1734–1739 (2017).
81. K. Wang, M. Li, H. Hakonarson, ANNOVAR: Functional annotation of genetic variants from high-throughput sequencing data. *Nucleic Acids Res.* **38**, e164 (2010).
82. L. D. Ward, M. Kellis, HaploReg: A resource for exploring chromatin states, conservation, and regulatory motif alterations within sets of genetically linked variants. *Nucleic Acids Res.* **40**, D930–D934 (2012).
83. A. P. Boyle, E. L. Hong, M. Hariharan, Y. Cheng, M. A. Schaub, M. Kasowski, K. J. Karczewski, J. Park, B. C. Hitz, S. Weng, J. M. Cherry, M. Snyder, Annotation of functional variation in personal genomes using RegulomeDB. *Genome Res.* **22**, 1790–1797 (2012).
84. GTEx Consortium, Human genomics. The Genotype-Tissue Expression (GTEx) pilot analysis: Multitissue gene regulation in humans. *Science* **348**, 648–660 (2015).
85. D. Trabzuni, M. Ryten, R. Walker, C. Smith, S. Imran, A. Ramasamy, M. E. Weale, J. Hardy, Quality control parameters on a large dataset of regionally dissected human control brains for whole genome expression studies. *J. Neurochem.* **119**, 275–282 (2011).
86. W. McLaren, L. Gil, S. E. Hunt, H. S. Riat, G. R. Ritchie, A. Thormann, P. Flicek, F. Cunningham, The Ensembl variant effect predictor. *Genome Biol.* **17**, 122 (2016).

Acknowledgments: We thank all the participants and their families, as well as the many institutions and their staff that provided support for the studies involved in this collaboration. This study was supported by access to equipment made possible by the Hope Center for Neurological Disorders and the Departments of Neurology and Psychiatry at Washington University School of Medicine. Data used in the preparation of this article were obtained from the ADNI database (adni.loni.usc.edu). The investigators within ADNI contributed to the design and implementation of ADNI and/or provided data but did not participate in analysis or writing of this paper. A complete listing of ADNI investigators can be found at http://adni.loni.usc.edu/wp-content/uploads/how_to_apply/ADNI_Acknowledgement_List.pdf. ADNI is funded by NIH grant no. U01 AG024904 and Department of Defense award no. W81XWH-12-2-0012. ADNI is also supported by the National Institute on Aging, by the National Institute of Biomedical Imaging and Bioengineering, and through generous contributions from the following: AbbVie, Alzheimer's Association, Alzheimer's Drug Discovery Foundation, Araclon Biotech, BioClinica Inc., Biogen, Bristol-Myers Squibb Company, CereSpir Inc., Cogstate, Eisai Inc., Elan Pharmaceuticals Inc., Eli Lilly and Company, EuroImmun, F. Hoffmann–La Roche Ltd. and its affiliated company Genentech Inc., Fujirebio, GE Healthcare, IXICO Ltd., Janssen Alzheimer Immunotherapy Research & Development LLC, Johnson & Johnson Pharmaceutical Research & Development LLC, Lumosity, Lundbeck, Merck & Co Inc., Meso Scale Diagnostics LLC, NeuroRx Research, Neurotrack Technologies, Novartis Pharmaceuticals Corporation, Pfizer Inc., Piramal Imaging, Servier, Takeda Pharmaceutical Company, and Transition Therapeutics. The Canadian Institutes of Health Research is providing funds to support ADNI clinical sites in Canada. Private sector contributions are facilitated by the Foundation for the National Institutes of Health (www.fnih.org). The grantee organization is the Northern California Institute for Research and Education, and the study is coordinated by the Alzheimer's Therapeutic Research Institute at the University of Southern California. ADNI data are disseminated by the Laboratory for NeuroImaging at the University of Southern California. Data collection and sharing for this project was supported by DIAN (UF1AG032438) funded by the National Institute on Aging, the German Center for Neurodegenerative Diseases (DZNE), Raul Carrea Institute for Neurological Research (FLENI), partial support by the Research and Development Grants for Dementia from Japan Agency for Medical Research and Development, and the Korea Health Technology R&D Project through the Korea Health Industry Development Institute (KHIDI). This manuscript has been reviewed by DIAN Study investigators for scientific content and consistency of data interpretation with previous DIAN Study publications. We acknowledge the altruism of the participants and their families and contributions of the DIAN research and support staff at each of the participating sites for their contributions to this study. Study data were provided by the following sources: the Mayo Clinic Alzheimer's Disease Genetic Studies, led by N. Taner and S. G. Younkin (Mayo Clinic, Jacksonville, FL), using samples from the Mayo Clinic Study of Aging, the Mayo Clinic Alzheimer's Disease Research Center, and the Mayo Clinic Brain Bank. Data collection was supported through funding by National Institute on Aging grants P50 AG016574, R01 AG032990, U01 AG046139, R01 AG018023, U01 AG006576, U01 AG006786, R01 AG025711, R01 AG017216, and R01 AG003949; NINDS grant R01 NS080820; the Cure PSP Foundation; and support from the Mayo Foundation. Study data include samples collected through the Sun Health Research Institute Brain and Body Donation Program of Sun City, Arizona. The Brain and Body Donation Program is supported by the National Institute of Neurological Disorders and Stroke (U24 NS072026 National Brain and Tissue Resource for Parkinson's Disease and Related Disorders), the National Institute on Aging (P30 AG19610 Arizona Alzheimer's Disease Core Center), the Arizona Department of Health Services (contract no. 211002, Arizona Alzheimer's Research Center), the Arizona Biomedical Research Commission (contract nos. 4001, 0011, 05-901, and 1001 to the Arizona Parkinson's Disease Consortium), and the Michael J. Fox Foundation for Parkinson's Research. Data for this study were generated from postmortem brain tissue collected through the Mount Sinai VA Medical Center Brain Bank and were provided by Eric Schadt from Mount Sinai School of Medicine.
Funding: This work was supported by grants from the NIH [R01AG044546 (to C.C.), P01AG003991 (to C. Cruchaga), RF1AG053303 (to C. Cruchaga), RF1AG058501 (to C. Cruchaga), U01AG058922 (to C. Cruchaga), K01AG046374 (to C.M.K.), and R01HL119813 (to T.J.B.)]. C. Cruchaga was also supported by the Alzheimer's Association (NIRG-11-200110, BAND-14-338165, AARG-16-441560, and BFG-15-362540). Y.D. was supported by an NIMH institutional training grant (T32MH014877). L.P. was supported by a grant from the Fondazione Italiana Sclerosi Multipla (FISM 2017/R/20). F.F. was supported by a Fondazione Veronesi fellowship. C. Cantoni was supported during the course of this study by a fellowship from the National Multiple Sclerosis Society (FG 2010-A1/2). B.A.B. is supported by 2018 pilot funding from the Hope Center for Neurological Disorders and the Danforth Foundation Challenge at Washington University. The recruitment and clinical characterization of research participants at Washington University was supported by NIH P50 AG05681, P01 AG03991, and P01 AG026276. K.B. holds the Torsten Söderberg Professorship in Medicine at the Royal Swedish Academy of Sciences. K.B. is also supported by grants from the Swedish Alzheimer's Foundation (no. AF-742881); the Research Council, Sweden (no. 2017-00915); Hjärnfonden, Sweden (no. FO2017-0243); and LUA/ALF project, Västra Götalandsregionen, Sweden (no. ALFGBG-715986). H.Z. is a Wallenberg Academy Fellow and is supported by grants from the Swedish and European Research Councils and the UK Dementia Research Institute at University College, London. C.H. was supported by the Deutsche Forschungsgemeinschaft

(DFG) within the framework of the Munich Cluster for Systems Neurology (EXC 1010 SyNergy), a DFG-funded Koselleck Project (HA1737/16-1), the NOMIS foundation, and the Frontotemporal Dementia Biomarker Award. **Author contributions:** Y.D. analyzed the GWAS data, performed bioinformatics analyses, and wrote the manuscript. F.F., F.C., C. Cruchaga, S.H., L.P., and C.M.K. designed and performed the cell-based studies. Z.L., J.L.D.-A., U.D., J. Bradley, B.A.B., and O.H. performed the gene expression analyses in human brain tissue. F.G.F., L.I., M.V.F., and J. Budde performed the QC for the GWAS data. K.B., H.Z., J.S., B.N., A.L., D.A., J.C., L.R., J.L.M., E.M.-R., and G.K. provided CSF TREM2 and genetic material for the replication analyses. M.S.-C., C.H., Y.D., L.P., and C. Cruchaga measured and performed quality control of the CSF sTREM2 in the ADNI dataset. L.P., C.M.K., and C. Cruchaga supervised and wrote the paper. All authors read and approved the manuscript. **Competing interests:** C. Cruchaga receives research support from Biogen, EISAI, and Alector and Parabon and is a member of the advisory board of ADx Healthcare, Halia Therapeutics, and Vivid Genomics. K.B. has served as a consultant or on advisory boards for Alzheon, BioArctic, Biogen, Eli Lilly, Fujirebio Europe, IBL International, Merck, Novartis, Pfizer, and Roche Diagnostics and is a co-founder of Brain Biomarker Solutions in Gothenburg AB, a GU Ventures–based platform company at the University of Gothenburg. H.Z. has served on scientific advisory boards for Eli Lilly, Roche Diagnostics, and Wave; has received travel support from Teva; and is a co-founder of Brain Biomarker Solutions in Gothenburg AB, a GU Ventures–based platform company at the University of Gothenburg. C.H. is a coinventor on patent no. PCT/EP2017/068684 entitled "Trem2 cleavage modulators and uses thereof." **Data and materials availability:** All data associated with this study are present in the paper or the Supplementary Materials. The data and phenotypes used in this study are available on the NIA Genetics of Alzheimer's Disease Storage Site (www.niagads.org/) under accession no. NG00089. The results from the GWAS analyses can be interactively explored in the Online Neurodegenerative Trait Integrative Multi-Omics Explorer (ONTIME) browser (http://ngi.pub:5000/). All ADNI data (GWAS, epidemiological, and CSF TREM2) are available through the LONI Image & Data Archive. Interested scientists may apply for access on the ADNI website (http://adni.loni.usc.edu/data-samples/access-data/). Samples and clinical information for the Knight-ADRC cohort are available to qualified investigators by applying through the Knight ADRC website (https://knightadrc.wustl.edu/Research/ResourceRequest.htm). Samples and clinical information for the DIAN cohort can be obtained by applying through the DIAN website (https://dian.wustl.edu/our-research/observational-study/dian-observational-study-investigator-resources/). Samples and clinical information for the following cohorts can be obtained from the principal investigators listed in parentheses: Sahlgrenska Academy at the University of Gothenburg (K.B. and H.Z.); the Memory Unit and Alzheimer's laboratory at the Hospital of Sant Pau, Barcelona (A.L.); and the ICN Hospital Clinic, Barcelona (J.L.M.).

Submitted 24 May 2018
Accepted 5 April 2019
Published 14 August 2019
10.1126/scitranslmed.aau2291

Citation: Y. Deming, F. Filipello, F. Cignarella, C. Cantoni, S. Hsu, R. Mikesell, Z. Li, J. L. Del-Aguila, U. Dube, F. G. Farias, J. Bradley, J. Budde, L. Ibanez, M. V. Fernandez, K. Blennow, H. Zetterberg, A. Heslegrave, P. M. Johansson, J. Svensson, B. Nellgård, A. Lleo, D. Alcolea, J. Clarimon, L. Rami, J. L. Molinuevo, M. Suárez-Calvet, E. Morenas-Rodríguez, G. Kleinberger, M. Ewers, O. Harari, C. Haass, T. J. Brett, B. A. Benitez, C. M. Karch, L. Piccio, C. Cruchaga, The *MS4A* gene cluster is a key modulator of soluble TREM2 and Alzheimer's disease risk. *Sci. Transl. Med.* **11**, eaau2291 (2019).

Science Translational Medicine

The *MS4A* gene cluster is a key modulator of soluble TREM2 and Alzheimer's disease risk

Yuetiva Deming, Fabia Filipello, Francesca Cignarella, Claudia Cantoni, Simon Hsu, Robert Mikesell, Zeran Li, Jorge L Del-Aguila, Umber Dube, Fabiana Geraldo Farias, Joseph Bradley, John Budde, Laura Ibanez, Maria Victoria Fernandez, Kaj Blennow, Henrik Zetterberg, Amanda Heslegrave, Per M Johansson, Johan Svensson, Bengt Nellgård, Alberto Lleo, Daniel Alcolea, Jordi Clarimon, Lorena Rami, José Luis Molinuevo, Marc Suárez-Calvet, Estrella Morenas-Rodríguez, Gernot Kleinberger, Michael Ewers, Oscar Harari, Christian Haass, Thomas J Brett, Bruno A. Benitez, Celeste M. Karch, Laura Piccio and Carlos Cruchaga

Sci Transl Med **11**, eaau2291.
DOI: 10.1126/scitranslmed.aau2291

TREM2 takes center stage

Genetic variants in triggering receptor expressed on myeloid cells 2 (*TREM2*) are associated with Alzheimer's disease (AD) risk. Soluble TREM2 (sTREM2) concentrations in cerebrospinal fluid (CSF) change with AD progression; however, genetic modifiers of CSF sTREM2 remain unknown. Deming and colleagues now report two independent genetic associations in the membrane-spanning 4-domains subfamily A (*MS4A*) gene region. An AD risk variant was associated with reduced CSF sTREM2 concentrations, whereas a different variant leading to reduced AD risk was associated with elevated CSF sTREM2 concentrations. Gene expression analyses and molecular studies of human macrophages validated a functional relationship between MS4A4A and sTREM2 concentrations.

Science Translational Medicine (ISSN 1946-6242) is published by the American Association for the Advancement of Science, 1200 New York Avenue NW, Washington, DC 20005. The title *Science Translational Medicine* is a registered trademark of AAAS.